Delivery of genetic material with virus-like particles

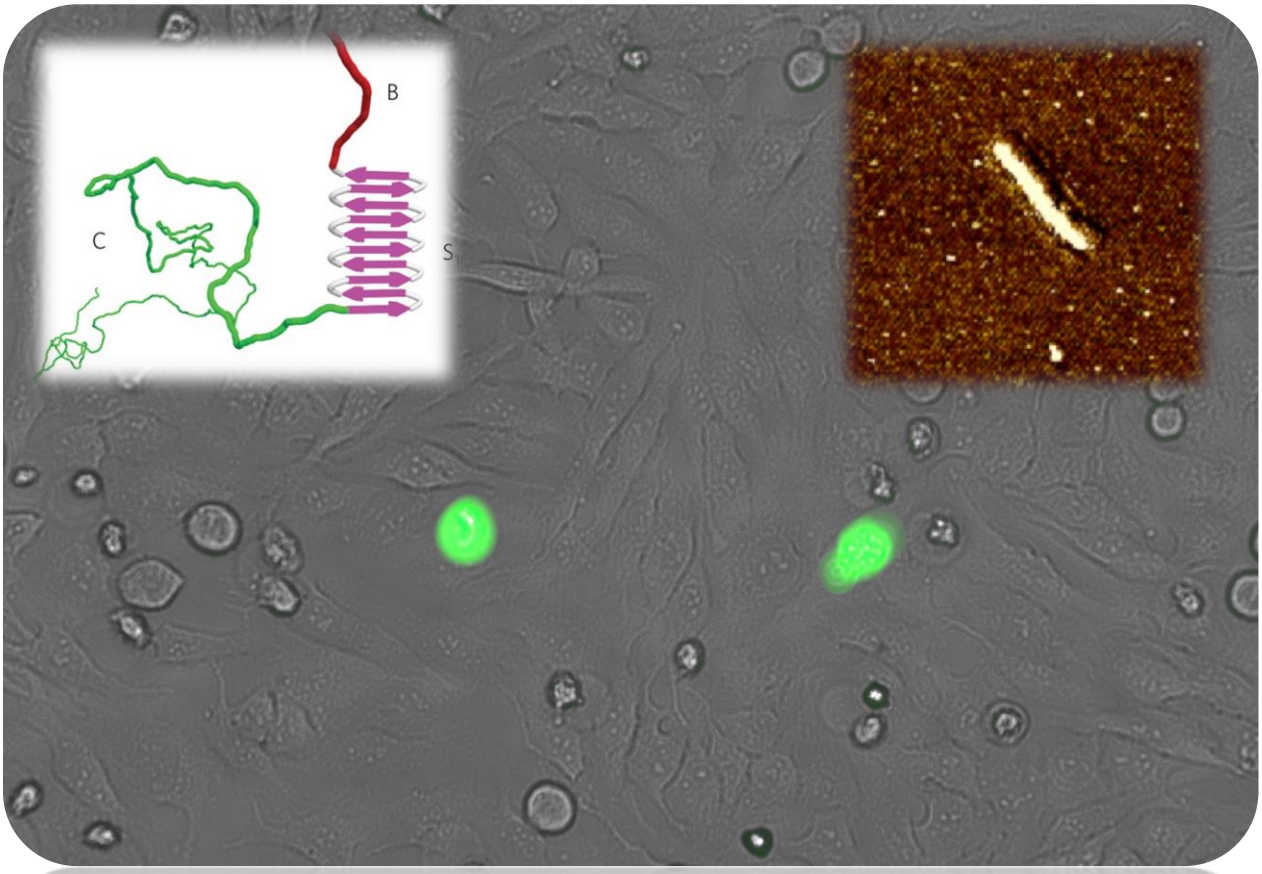

MSc Thesis
Hanna de Jong
930321402010
Molecular Life Sciences, Physical chemistry
Supervisors:
dr. RJ de Vries
Laboratory for Physical Chemistry and Soft Matter
dr. EJ Tijhaar
Laboratory for Cell Biology and Immunology
May 2016

1 Abstract

Targeted delivery of genetic material with viral and non-viral systems is challenging because of the many barriers that must be faced. Previously, a system was designed based on the cooperative behaviour of a viral coat protein forming virus-like particles. In this thesis, the barriers for the virus-like particles are explored. First, the transfection efficiency was studied and was found to be much lower than previous results indicated, or compared to the positive control. The viral coat protein was modified with a fluorophore and an adhesion motif, a peptide containing an RGD sequence. With these modified proteins the cell uptake could be studied. A transfection study was performed with the fluorescently labelled particles that indicated that almost every cell had taken up a particle, but it remained unclear whether the fluorescence signal originated from loose protein or aggregates. However, the experiment demonstrated the power of flow cytometry to quantify the uptake level. The potential of flow cytometry was again illustrated with the detection of a few GFP-expressing cells transfected with RGD modified VLPs. Finally, to get an indication of the immunogenicity of the VLPs, the effect on these particles on the activation and maturation of dendritic cells (DCs) was studied. The data gave a strong indication that the particles could be tolerated by the body which is useful for its application in therapy. In summary, several barriers towards the delivery of genetic material with virus-like particles were successfully explored. Moreover a set of techniques, including chemical modification of the C4SQ10K12 protein and analysis of cell uptake by flow cytometry, was used that is also applicable to any further studies on the transfection with virus-like particles.

2 Table of content

3 List of abbreviations

AAV	=adeno-associated vector
AFM	=atomic force microscopy
APC	=antigen-presenting cell
BSA	=bovine serum albumin
C4SQ10K12	=viral coat protein
CD	=cluster of differentiation
Da	=dalton, mass unit
DC	=dendritic cell
DLS	=dynamic light scattering
DNA	=deoxyribonucleic acid
DTT	=dithiothreitol
eGFP	=enhanced green fluorescent protein
EtOH	=ethanol
GFP	=green fluorescent protein
FACS	=fluorescence activated cell sorting
FBS	=fetal bovine serum
FC	=flow cytometry
FCS	=fetal calf serum
GALA	=30 amino acid long peptide
HEK	=human embryonic kidney
HeLa	=cervical cancer cells taken from Henriette Lacks
LPS	=lipopolysaccharide
MALDI-TOF	=matrix assisted laser desorption ionization- time of flight
MHC	=major histocompatibility complex
mRNA	=messenger ribonucleic acid
NsiI	=restriction enzyme
PB	=phosphate buffer
PBS	=phosphate-buffered saline
PEG	=poly-ethylene glycol
RGD	=arginine-glycine-aspartic acid
RNA	=ribonucleic acid
RT	=room temperature
SDS-PAGE	=sodium dodecyl sulfate polyacrylamide gel electrophoresis
SEC	=size exclusion chromatography
TFA	=trifluoroacetic acid
UV/VIS	=ultraviolet/visible spectroscopy
VLP	=virus-like particle

4 Introduction

4.1 Gene and immunotherapy

The delivery of genetic material, or more general polynucleotides, has great potential in controlling the level or activity of targeted proteins. Ultimately, efficient delivery of polynucleotides can be used as a precision tool for gene therapy or immunotherapy.

The promise of gene therapy was raised long ago, but its promise has not yet been fulfilled. The major goal of gene therapy is the safe delivery of the gene of interest into the targeted cell and a stable expression level of the gene of interest. In general, gene therapy has known several setbacks due to associated toxicity and expectations that were much too high.[1] Essential to achieving the goal of gene therapy is a safe vector for delivery.

Besides gene therapy delivery of polynucleotides can also be used for immunotherapy. Some diseases, like cancer, are known to induce a limited immune response.[2] An increased immune response is accomplished by targeting one of the key players of the immune system, the dendritic cell (DC). The DC scavenges for antigens, takes them up, processes them and presents them to other parts of the immune system (Figure 1). Because of its function, a DC is classified as a professional antigen-presenting cell (APC). The function of the DC provides the possibility to present parts of a tumour for which an immune response is needed. When a DC is loaded *ex vivo* with the tumour antigen and an individual is vaccinated with the loaded DC, the immune system can be boosted. Despite the promising application of DCs in immunotherapy, several challenges remain including the efficient delivery of antigen to the DC.[3]

Both for gene therapy and immunotherapy delivery of genetic material is required. In order to achieve efficient transport to a cell vectors can be used.

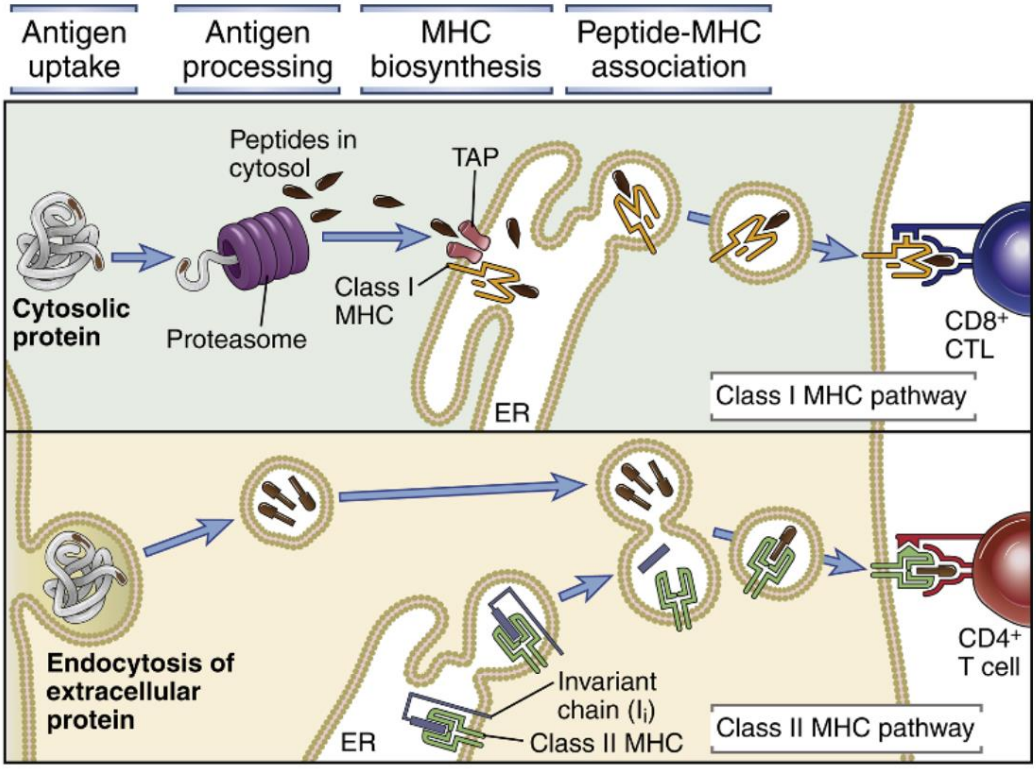

Figure 1. Schematic overview of antigen presentation via class I and II MHC (Major HistoCompatibility) pathway. When a protein is present in the cytosol and degraded by the proteasome the antigen is presented via MHC I (top). When the antigen is taken up via endocytosis and degraded in the endosomes, the antigen is presented via MHC II (bottom). In both cases parts of the immune system are activated. Adapted from Abbas et al.[4]

4.2 Viral and non-viral vectors

Delivery vehicles for polynucleotides can be separated into viral and non-viral vectors. Moreover, viral vectors have a subclass of retroviral vectors, for example Mouse Moloney retroviruses and Lentiviral vectors. These complexes can be made to infect dividing mammalian cells and non-dividing cells, respectively. Although both vectors have made it to clinical trials, the safety remains a concern and the potential oncogenic risk is unknown. Another type of viral vector is the adenoviral vector which allows for the insertion of relatively large sequences into its genome. Despite the promising results for gene transfer, the adenoviral vectors might have limited applications due the origin of the vector: the vector is derived from so-called, adenovirus type 5. Most adults have been exposed to this particular type and therefore have acquired immunity. Unlike adenoviral vectors, adeno-associated vectors (AAVs) can be transformed into another type and can circumvent the problem of acquired immunity. AAVs differ from there associated partners because they require a helper virus for replication and their life cycle. AAVs are promising delivery vehicles and clinical trials can either confirm or oppose this.[5]

Non-viral vectors have some advantages over viral vectors: potential low immunogenicity, loading capacity and ease of manufacturing. A well-known example of a non-viral vector is the cationic lipid-based formulation Lipofectamine which has a good transfection efficacy. In addition, vectors like lipid-DNA (lipoplexes) and polymer-DNA (polyplexes) rely on the same electrostatic interaction between the cationic lipids or polymers and the negative charge of the phosphate groups in DNA.[6] Other types of non-viral vectors include dendrimers, neutral lipids and combinations of lipids and polymers (Figure 2).[7] The research into synthetic vectors highlights an important problem: the mechanism of action is not always known for these vectors and therefore should be studied in order to prevent toxic effects. Indeed, some cationic lipids and polymers have suspected toxicity.[8]

In short, viral vectors have good efficacy and some are already clinically tested, but they can evoke an undesired immune response, have limited loading capacity and suffer from safety concerns. In contrast, non-viral vectors have a low efficacy and the mechanism of action is not always known, but they potentially have low immunogenicity, high loading capacity and are easily manufactured.[5, 9] In search of the ultimate delivery vehicle, a non-viral vector mimicking the behaviour of a virus could combine best of both worlds. However, the introduction of polynucleotides with any kind of vector is not straightforward and has yet several barriers to overcome before becoming a widespread application.

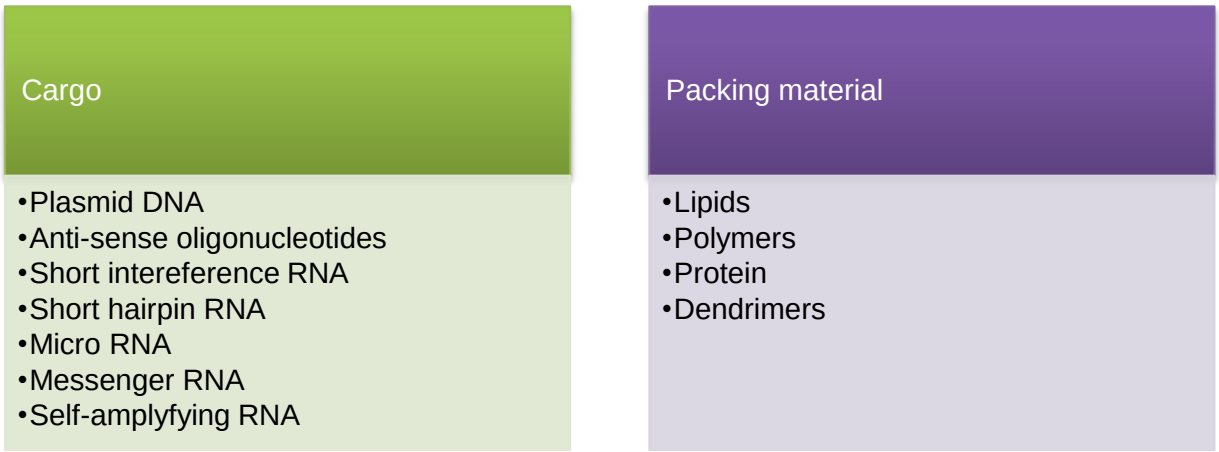

Figure 2. Overview of components composing non-viral vectors. [6, 7, 10, 11, 12, 13, 14]

4.3 Barriers to efficient delivery

There are several barriers a vector must overcome in order to effectively deliver genetic material inside the cell (Figure 3). First, a vector should elicit the desired immune response with regard to its application. In the extreme case, the immune system can react in two ways: either the immune system tolerates the delivery vehicle or elicits an immune response consisting of the release of cytokines, activation of CD8+ and/or CD4+ T cells and the production of memory cells.[10] Both type of reactions of the immune system can be wanted and are dependent on the goal of administering a vector. In case you want to immunize directly against the material you are injecting, the activation of the immune system is desired. However, usually tolerance is aimed for, because it allows for repetitive administration of the same type of vector. This problem was briefly touched upon for the adenoviral vector, which is not effective due to pre-existing immunity.[5] A second hurdle to overcome is extracellular degradation by nucleases.[15] The genetic material must stay protected while the vector travels through the body. A third challenge arises when the particle moves inside the body and that is the targeted delivery to a specific cell type. The affinity of the delivery vehicle for a cell type is referred to as tropism.[16] The tropism of a vector can be altered by attaching cell specific moieties or using gene promoters that are only active in certain cell types.[10, 16, 14] After reaching the targeted cell type, the vector must be taken up by the cell, for example via endocytosis. Once inside the cell, the particle must escape from the endosomal compartment to the cytosol. Otherwise, the content of the compartment is degraded in a lysosome. This fifth step is indicated as a major hurdle for delivery and sometimes pointed to as the rate-limiting step. Notably, Bieber et al.[17] demonstrated that for the non-viral vector, PEI-DNA the transfection efficiency was only 20% while the complexes accumulated in the lysosomes. Furthermore, their work indicated that the unpacking of non-viral vectors could be another hurdle. Interestingly, they found that complexed PEI-DNA can be transcribed and that the complexed form is more efficiently transported from the cytosol to the nucleus than the naked genetic material.[17] Additionally, the naked genetic material must be stable while present in the cytosol. Moreover, the stability must remain while the polynucleotides are transported to the nucleus in case of DNA.[15] The final barrier is the transport to the site of action in the cell which poses the hurdle of crossing the nuclear envelope for DNA.[10, 14]

In summary, each vector independent of origin must overcome the following barriers: elicit the desired immune response, extracellular degradation, targeting a specific cell type, uptake across the cell membrane, endosomal escape, cytosolic degradation and transport of polynucleotides to the site of action. The amount and complexity of these challenges requires a smart and tuneable design.

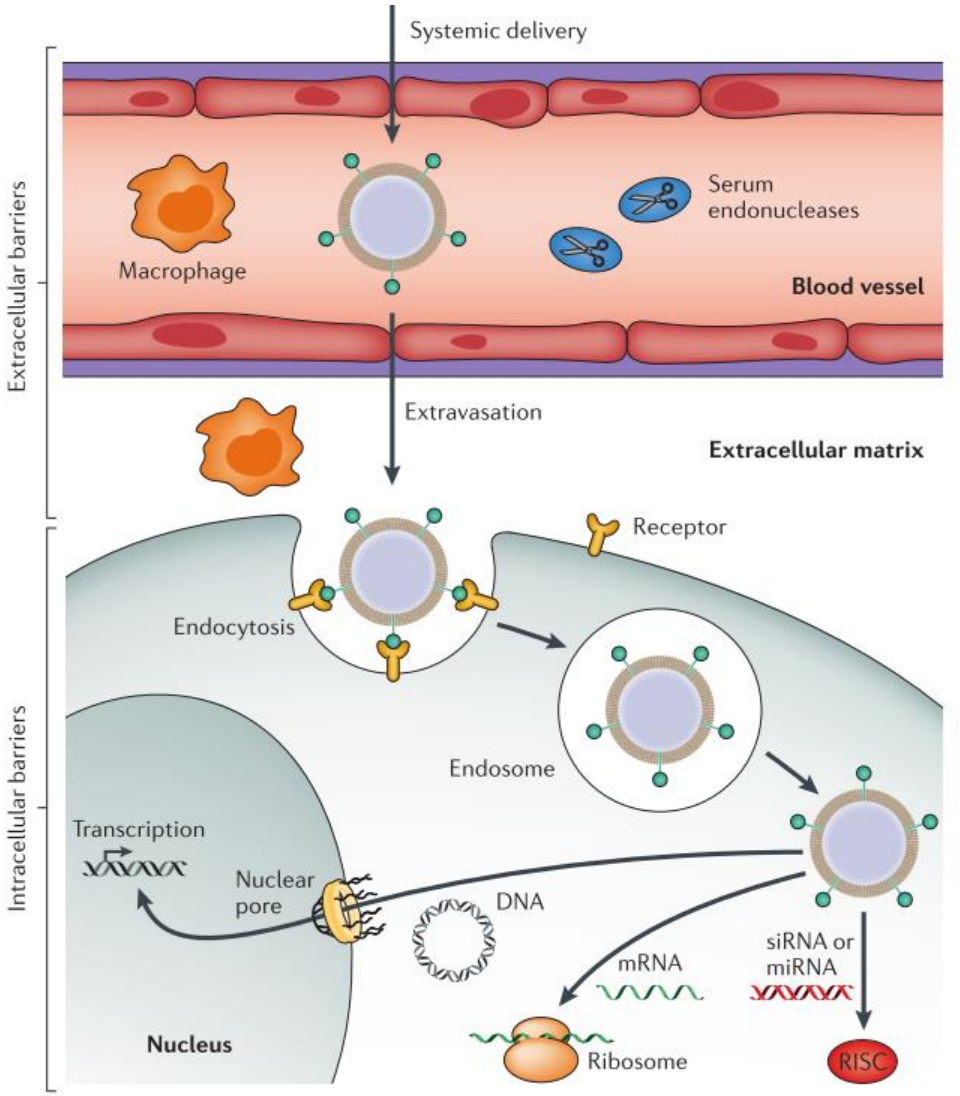

Figure 3. Schematic overview indicating some of the challenges a vector faces: elicit the desired immune response, extracellular degradation, uptake across the cell membrane, endosomal escape and transport to the nucleus. Adapted from Yin et al.[14]

4.4 Design of an artificial virus

Recently, a design for a protein that can self-assemble with DNA into virus-like particles (VLPs) was reported.[13] Based on the cooperative self-assembly behaviour of tobacco mosaic virus coat proteins onto nucleic acids, an artificial coat protein was designed with three functional domains (Figure 4)[13]. The structure of the protein allows for multiple modifications as discussed later and therefore the system has excellent options in overcoming the barriers to successful delivery.

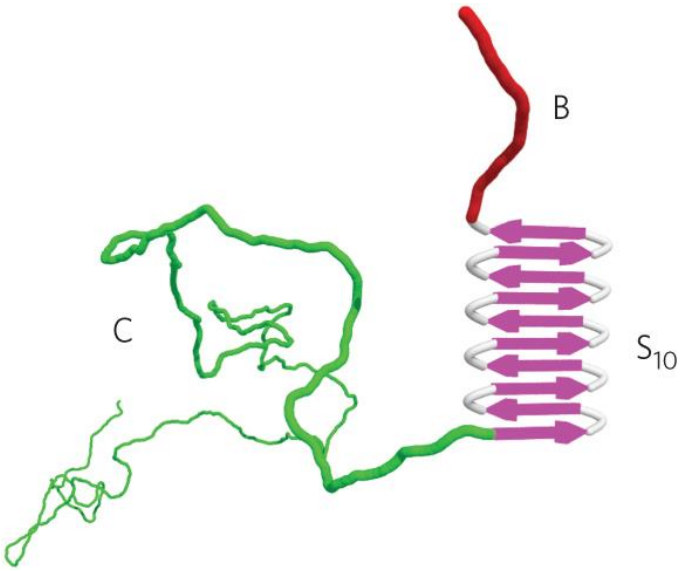

Figure 4. Design of a coat protein for the assembly into artificial viruses. The protein constitutes three different blocks with B=K_{12} as DNA binding domain, SQ10 as cooperative element and C as an inhibitor of the aggregation of VLPs.

The DNA binding domain is composed of twelve positively charged lysine moieties which give rise to the electrostatic attraction with the negatively charged phosphate groups of the DNA. A tenfold silk-like sequence, S_{10}=$(GAGAGAGQ)_{10}$ enables the cooperative assembly of the coat proteins on the template. At the end, a random-coil sequence C is incorporated to prevent aggregation of the VLPs themselves. The designed coat protein resembles the assembly into a virus, like the tobacco mosaic virus. Furthermore, it was demonstrated that the nucleic acid cargo is protected against enzymatic attack. Moreover, the DNA-protein complexes were used to transfect HeLa cells.[13]
The designed protein C4SQ10K12 assembles around genetic material forming a virus-like particle, which is the focus of this research. As discussed previously a vector faces many challenges which will be explored for this non-viral vector. Especially, the transfection capability of the artificial viruses could be improved in light of combining the best properties of viral and non-viral vectors.

4.5 Improving the transfection efficiency

A major step into reaching the same transfection level as viruses must be accomplished for the effective polynucleotide delivery of non-viral vectors in general.[9] Likewise, the designed artificial viruses of genetic material with C4SQ10K12 protein leave room for promoted cellular uptake.
In order to achieve increased uptake of the VLPs, an adhesion motif that sticks to the cell can be used. The adhesion motif can be covalently coupled to the protein. However, the first hurdle presents itself which is the assembly of the protein in solution during a chemical reaction. Therefore, a means to disassemble the formed aggregates is required. Thus, prior to testing chemical coupling the disassembling conditions of the proteins are determined. With this information in hand, protein aggregates formed during the chemical coupling can be separated into monomers again, which then can be used to form modified VLPs. The disassembling properties are tested for a chaotropic salt, urea or heat.[18, 19]
Hereafter, a bio conjugation reaction is tested to couple a targeting moiety to the viral coat protein. Fortunately, the last two amino acids of the random-coil domain C constitute a cysteine and a terminal glycine which allow for several chemical approaches. An excellent method to couple a targeting moiety to the cysteine of the viral coat protein is a thiol-Michael addition reaction employing a thiol and maleimide (Scheme 1). The reaction is stereospecific, can give high yields, generates little by-products and can be performed without solvent.

Therefore, the reaction is sometimes referred to as a “click” reaction.[20, 21] Furthermore, the reaction is often used for biological applications, because it can be performed in water.[20, 22]

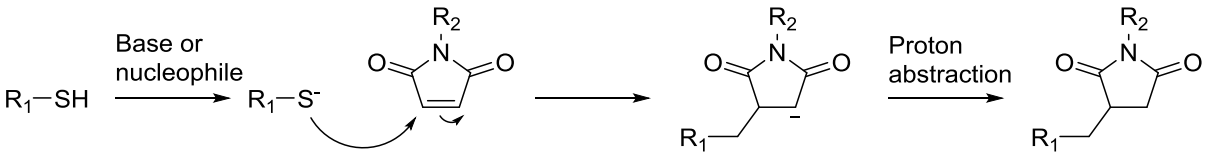

Scheme 1. Proposed reaction mechanism for the thiol- Michael reaction. The thiol, originating from the cysteine of the protein gets deprotonated and attacks the double bond of the maleimide-group. After abstraction of a proton, the coupling is finished

The thiol-Michael reaction will be tested with a red fluorescent dye connected to a maleimide (Figure 5). Besides testing the conjugation, the modified proteins can be used to track the fluorescently labelled VLPs.

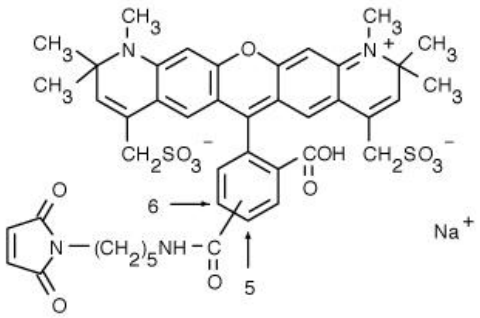

Figure 5. Structure of Alexa Fluor 594; a red fluorescent dye used to modify the protein C4SQ10K12.

An alternative option for the thiol-Michael addition is the conversion of the cysteine from the viral coat protein into a dehydroanaline and coupling to the targeting moiety via a thiol containing compound.[23]

Once the chemical conjugation is established, targeting peptides are explored to increase the overall uptake in HeLa cells. A well-known adhesion motif is the RGD sequence (R=arginine, G=glycine and D=aspartic acid) which can be surrounded by a variety of different amino acids and maintaining its property.[24, 25, 26, 27 28] For example, RGD, RGDS (additional serine), RGDV (additional valine), RGDT (additional threonine) which were all connected to a polymer are known to have an effect on HeLa cells.[29] For this study, an adhesion motif that was previously employed in our lab was chosen and slightly adjusted to incorporate the maleimide functionality (Figure 6).[30] Ultimately, the transfection efficiency of non-viral vectors equals or outreaches the sophisticated level of viruses and the targeting can be tuned via selective peptides, for instance the NW peptide which is selective for dendritic cells.[31]

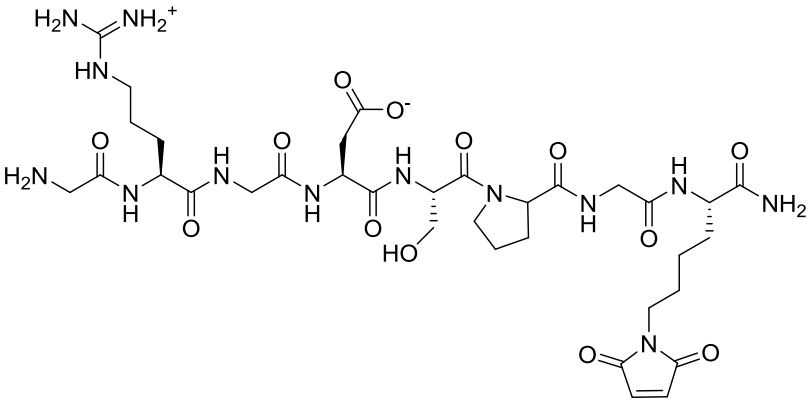

Figure 6. RGD motif chosen for promoted cellular uptake. The peptide sequence consists of H-Gly-Arg-Gly-Asp-Ser-Pro-Gly-Lys(Mal)-NH2.

4.6 Endosomal escape

Another important step for efficient delivery of genetic material is the development of an element which is responsible for the endosomal escape of the vector into the cytosol. A first step towards constructing an escape element requires knowledge about the trafficking of the vector. Several methods for endocytosis exist dependent on the cell type (Figure 7)[32], but dendritic cells make use of all of them. Therefore, dendritic cells are an outstanding test subject for testing the endocytic pathway, as previously illustrated for a lipoplex vector by Haes et al.[33] Often, when a vector is taken up it is transported in a endosome or lysosome. Within the endosomal compartment, a pH change takes place and this change in environment can be used for the design of an escape element. The 30 amino acid long GALA peptide benefits from the pH drop as the repulsive interaction between the negatively charged glutamic acids disappear due to protonation. Therefore, the GALA peptide undergoes a conformational change into a helical structure which can interact with the endosomal membrane.[34] The positioning of the GALA peptide alters the activity drastically and the peptide must be displayed on the surface of the vector and not encapsulated inside in order to promote endosomal escape.[35] GALA is a well-known endosomal escape element and has been used in combination with several nanocarriers.[36, 37, 38] Another cell-penetrating peptide is TAT (transactivator of transcription) which originates from HIV. The protein likely promotes endosomal escape after cellular uptake via energy-dependent macropinocytosis.[39] An exact mechanism of action for TAT is not known, but research indicated that the protein promotes uptake via macropinocytosis leading to macropinosomes which are known to be leaky.[40] Therefore, TAT could promote endosomal escape at the first cellular barrier, namely uptake. Similar to GALA, several molecules attached to TAT were used to increase the delivery inside the cell.[41, 42, 43]

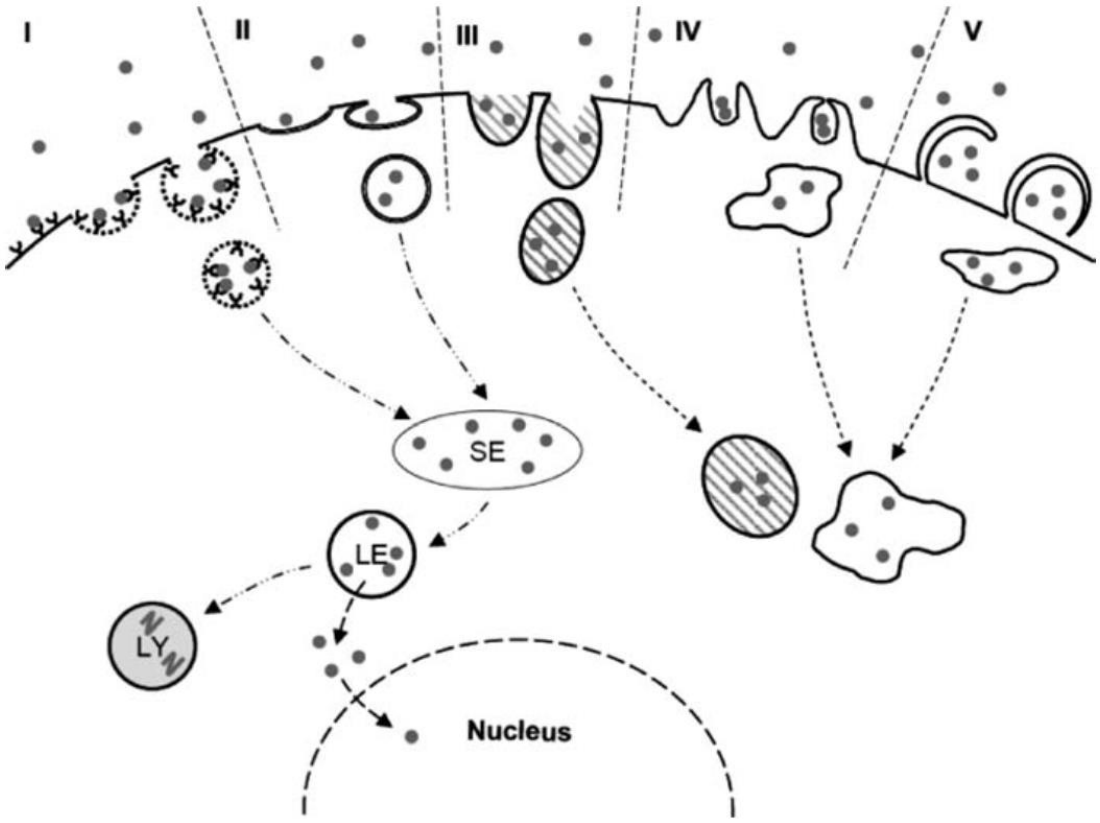

Figure 7. Overview of endocytic pathways in a cell. I Clathrin-dependent endocytosis, II lipid raft/membrane microdomain, III caveolin-dependent endocytosis, IV phagocytosis, V macropinocytosis. SE=sorting endosome, LE=late endosome and LY=lysosome. Molecules are enzymatically and acidically degraded in the lysosome. Adapted from Douglas et al.[9]

5 Aim of this study

The aim of this study is to explore the barriers for efficient delivery of genetic material to the targeted cell with an artificial virus consisting of C4SQ10K12 protein and polynucleotides. In particular, transfection studies will be performed to reproduce previously obtained results and possibly increase the transfection efficiency. Furthermore, the disassembly conditions are sought for the protein in order to disassemble any formed aggregates of protein. C4SQ10K12 will be chemically labelled with a fluorophore to test the method for conjugation. Additionally, the particle formation with the fluorescently labelled protein will be tested and the modified particles will be tracked during a localization study. Moreover, the protein will be modified with a RGD peptide to achieve increased transfection efficiency. Finally, the immunogenicity of the VLPs and protein will be explored.

6 Material and methods

For a detailed experimental description of all experiments, the reader is referred to the electronic lab journal.

6.1 Chemicals

Commercially obtained chemicals are used without further purification unless stated otherwise. Enhanced Green Fluorescent Protein mRNA (eGFP mRNA) was commercially obtained from TriLink Biotechnologies. The eGFP mRNA (996 nucleotides, 1.0mg/mL in 10mM Tris-HCl pH7.5) is capped and polyadenylated to mimic mature mRNA. Plasmid DNA encoding for GFP protein, pmax GFP DNA (3486 nucleotides, c=519ng/µL), was provided by the Cell Biology and Immunology laboratory. The protein, C4SQ10K12 was kindly provided by R. de Vries and was previously produced as described in literature.[13] Lipofectamine and Alexa Fluor 594 c5 maleimide were purchased from Fischer Scientific and Life Technologies, respectively. The RGD-containing peptide with a maleimide functionality (sequence: H-GRGDSPGK(Mal)-NH2) was ordered from PepScan, Lelystad.

6.2 RNA-protein complex formation

The protein, C4SQ10K12 was dissolved in filtered milliQ in an RNase free tube. Subsequently, the solution was vortexed for about a minute and centrifuged briefly if foam or bubbles appeared. The mixture was heated at 65°C for ten minutes and again vortexed for a minute and centrifuged briefly. EGFP mRNA was thawed on ice, divided in aliquots and 1 µL was diluted with a 10mM PB buffer containing 0.1mM DTT to reach a final RNA concentration of 1 µg/mL. The appropriate amounts of RNA- and protein stock solution are mixed by pipetting up and down to gain a N/P ratio of 3 (N indicates the positively charged amine groups of the lysine, K_{12}, and P indicates the negatively charged phosphate groups of the mRNA). The sample was left to incubate for 24 hours at room temperature.

6.3 DNA-protein complex formation

The protein, C4SQ10K12 was dissolved in filtered milliQ. The solution was vortexed for about a minute and centrifuged briefly if foam or bubbles appeared. The mixture was heated at 65°C for ten minutes and again centrifuged briefly. Pmax GFP DNA was added to reach a N/P ratio of 3 or 6 (N indicates the positively charged amine groups of the lysine, K_{12}, and P indicates the negatively charged phosphate groups of the DNA). The sample was carefully mixed and left to incubate for 24 hours at room temperature.

6.4 Atomic Force Microscopy

Atomic Force Microscopy (AFM) was used to confirm the aggregation of RNA/DNA and protein into virus-like particles. AFM images were recorded on Digital Instruments Nanoscope V with a non-conductive silicon nitride probe (Bruker) with a spring constant of 0.4 N/m in the ScanAssyst mode in air. Silicon wafers of approximately 1 x 1 cm were prepared by sonicating these in 96% ethanol solution, drying with a tissue and nitrogen flow and then plasma cleaning for 2 minutes. Samples were prepared by applying 10 µL of solution onto the silicon wafer, waiting for 2-3 minutes, rinsing with 1 mL milliQ in order to remove salts or unabsorbed material and drying by nitrogen flow. AFM images were analysed with NanoScope analysis 1.40 software.

6.5 Dynamic Light Scattering

Dynamic Light Scattering (DLS) was used to observe complexes of protein and RNA/DNA or protein only. Furthermore, DLS was used to demonstrate the assembly and disassembly of aggregates over time. The intensity was measured under a 173° angle on Malvern Instruments ZEN3600. A quartz cuvette was used and the data was visualized with Zetasizer software. Data was exported and processed with Microsoft Excel.

6.6 Size Exclusion Chromatography

Size Exclusion Chromatography (SEC) was performed to separate protein monomers from complexes and to confirm the disassembly of aggregates. SEC was performed on a BioLogic DuoFlow (BioRad) connected to a BioLogic QuadTec UV-VIS detector. The column was either a Superdex 200 or Superdex 75. All samples were filtered with centrifugal filters (0.22µm, Millipore) prior to injecting. Data was exported and plotted in excel.

6.7 Fluorescent labelling

The protein, C4SQ10K12 was fluorescently labelled with Alexa Fluor 594. A molar excess DTT was dissolved in PB buffer (50mM, pH=7.5). The protein was dissolved in PB buffer containing DTT and incubated for one hour at RT. The sample was transferred to 3kDa filters and centrifuged four times in total at 13000xg for 10 minutes while washing with milliQ. To a cleaned flask which was covered in aluminium foil and capped with argon, the protein solution was added. The fluorophore was dissolved in anhydrous DMSO and added to the stirring protein solution. After 2 hours, the reaction mixture was transferred to 3kDa filters and centrifuged four times in total at 13000xg for 5 or 10 minutes while washing with milliQ. The last filtrate was purple indicating that loose label might be present still in the protein solution. The sample was frozen for 30 minutes in liquid nitrogen and freeze dried for 22-40 hours to obtain a dark blue material.

6.8 RGD peptide labelling

The protein, C4SQ10K12 was labelled with a peptide containing a RGD sequence. A molar excess DTT (0.48mg) was dissolved in PB buffer (50mM, pH=7.5, 7.03mL). The protein(2.05mg) was dissolved in PB buffer with DTT (1mL) and incubated for one hour at RT. The sample was transferred to 3kDa filters and centrifuged five times over at 13000xg for 10 minutes. The protein solution was added to a cleaned flask which was capped with argon. The peptide (2mg) was dissolved in DMSO (1.1mL) and added to the stirring protein solution. After 2 hours, the reaction mixture was transferred to 3kDa filters and centrifuged six times in total at 13000xg for 15 minutes while washing with milliQ. The sample was frozen for 30 minutes in liquid nitrogen and freeze dried for 46 hours to obtain a white material.

6.9 SDS-PAGE

Sodium Dodecyl Sulphate PolyAcrylamide Gel Electrophoresis (SDS-PAGE) was performed to check the fluorescent labelling. C4SQ10K12 protein (0.4mg) was dissolved in 200µL mQ. A small amount of fluorescently labelled protein was dissolved in 100µL mQ. Both samples were vortexed for one minute and the concentration was determined with Nanodrop (A280). The concentration was 3.26mg/mL for the modified protein. However, the fluorescent group might contribute to the signal. The concentration for the unmodified protein was 0.10mg/mL, but the artificial protein might not absorb at 280nm. After heating for 10 minutes at 65°C, 50µL sample of both samples was taken and 10µL sample buffer was added. The samples were heated at 95°C for 5 minutes. The precasted gel (SDS-PAGE) was prepared, loaded and runned at 200V for approximately 20 minutes. A photo was taken prior to staining to observe the fluorescent groups by eye. The gel was washed three times for 15 minutes with demi-water and stained with coomassie blue. A photo was taken.

6.10 UV/VIS

Ultraviolet/visible spectroscopy (UV/VIS) was used to assess the labelling degree of the fluorescently labelled protein. A calibration curve was made for the fluorophore by dissolving alexa fluor 594 (0.31mg) in milliQ (c=0.15 mg/mL) and measuring a dilution series. A spectrum was recorded from 200 to 800nm with an integration time of 0.10s and 1nm

bandwidth. Similar settings were used to record spectra for a dilution series of fluorescently labelled protein starting from c=1mg/mL. Data was exported and plotted in excel.

6.11 MALDI-TOF

Matrix Assisted Laser Desorption Ionization- Time Of Flight (MALDI-TOF) (Bruker, UltrafleXtreme MALDI-TOF/TOF) was used to determine the mass of the labelled protein. Dihydroxyacetophenon (4.9mg) was dissolved in EtOH (214µL). Ammonium citric dibase (8.6mg) was dissolved in milliQ (478µL). The matrix (242µL) and base (81µL) were mixed for 1 hour. A 3% trifluoroacetic acid (TFA) solution was prepared in milliQ. The MALDI-TOF plate was excessively rinsed with hot water, cleaned with acetone and dried with a dust-free tissue. Each sample was mixed with TFA and matrix. When a milky substance was observed the sample was deposited on the plate. The samples dried on the plate within one hour. A mass spectrum was measured using a FBR method and suppressing masses up to 8 kDa.

6.12 Cell culturing

HeLa and HEK cells were cultured as monolayers in Advanced DMEM supplemented with L-glutamine, penicillin and streptomycin and 10%FBS. Cells were incubated at 37°C in a humidified atmosphere with 5% CO_2. Cells were passaged after 2 days or when reaching 80-90% confluency. Cells were seeded in a 24 well plate 24 hour prior to transfection at a density of $1x10^5$ cells/well/mL and incubated at 37°C in a humidified atmosphere with 5% CO_2.

6.13 Transfection

6.13.1 Transfection 1: initial search for conditions

The first transfection was performed for HeLa and HEK cells. The cells were seeded and the VLPs were made 24 hour prior to transfection. The medium of 24 well plates was replaced with 1mL fresh medium containing FCS (HeLa) and the other two with 1mL Opti-MEM (HeLa and HEK). To the cells nothing, naked plasmid, VLPs, lipoplexes (50µL), lipoplexes (4x less, 12.5µL) and milliQ was added. Lipoplexes were made according to optimized protocol; 1µg DNA in 50µL Opti-MEM and 2-5µg lipofectamine in 50µL Opti-MEM were mixed giving two samples. Different amounts of DNA and protein were added for the VLPs (Table 1).

Table 1. Amounts of C4SQ10K12 and pmax GFP DNA added as VLPs.

Sample volume (µL)	Protein (ng)	pDNA (ng)
60	3600	60.1
120	7200	120.2
180	10800	180.3
240	14400	240.4

After 3 hours, the Opti-MEM was changed for the HEK cells by FCS containing medium. All cells were incubated at 37°C in a humidified atmosphere with 5% CO_2 and the fluorescence was checked after 24 and 48 hour by fluorescence microscopy. AFM images were made of the VLPs that were used to transfect HeLa cells.

6.13.2 Transfection 2: improving transfection conditions

A second transfection was performed for HeLa cells which were seeded in 24 wells plates 24 hours prior to transfection. Two batches of VLPs were made, one in PB and the other in Opti-MEM with a constant amount of DNA and a varying amount of protein (Table 2). The VLPs and lipoplexes were added to the cells. After 24 hours, the fluorescence was observed with microscopy and the medium of the cells was changed for 1mL FBS containing Opti-MEM. Again, after 96 hours the fluorescence was checked with fluorescence microscopy.

Table 2. The amount of pmax GFP DNA was kept constant and the amount of C4SQ10K12 added as VLPs varied.

Sample volume(µL)	Protein (ng)	pDNA (ng)
75	1250-7250	32.4
150	2400-14500	64.9
300	5000-29000	130

6.13.3 Transfection 3: linear vs circular

A third transfection was performed for HeLa and HEK cells. VLPs were made with restricted and unrestricted pmax GFP DNA as well as unmodified protein and fluorescently labelled protein (Table 3). After 24 hours, the VLPs were corrected for salt concentration by adding filtered PBS (approximately 10x for the salt and 50x for the phosphates), but the dilutions were wrong. VLPs and lipoplexes were added to the cells and after 4 hours 1 mL FCS containing medium supplemented with the anti-fungal normicin was added. After 24 and 48 hours at 37°C in a humidified atmosphere with 5% CO_2, fluorescence microscopy was performed. Cells were analysed with flow cytometry.

Table 3. Amounts of protein and pmax GFP DNA added as VLPs. The protein is either unmodified or fluorescently labelled. The plasmid DNA is either linear or circular.

Sample volume(µL)	Protein (ng)	pDNA (ng)
4.95	2970	49.5
9.9	5940	99
19.8	11880	198
29.7	17820	297

6.13.4 Transfection 4: dendritic cells

A fourth transfection was performed for dendritic cells, which were kindly provided by Olaf Perdijk at a density of 100 000 cells/well in a 96 well plate. The DCs received a different kind of pre-treatment to study the effects of a pre-treatment on the level of uptake. However, in the end the effects could not be quantified, because there was minimal GFP expression as analysed by flow cytometry. The medium on top of the DCs was removed leaving 50µL behind. The cells were washed with an additional 150µL Opti-MEM. The plate was centrifuged at 400g for 3 min at 4°C. The medium was discarded and the VLPs were added in Opti-MEM (total volume was 90µL). The same amount of protein and DNA were added to DCs that received a different pre-treatment (Table 4). In contrast, DCs that did not receive any kind of pre-treatment or pre-treatment with SL mix were subjected to different amounts of protein and DNA in the form of VLPs (Table 5). After 3 hours, 100µL serum containing Opti-MEM was added on top of the medium present. The cells were further incubated at 37°C in a humidified atmosphere with 5% CO2. After 24 and 48 hours the fluorescence was checked with fluorescence microscopy. Moreover, after 48 hours the cells were prepared for flow cytometry analysis. The 96 well plate was put on ice for 30 min before the solution was suspended and transferred to another 96 well plate on ice. 200µL FACS buffer was added and the cells were suspended vigorously. The plate was centrifuged at 400g for 5 min at 4°C and the medium was discarded. The cells were washed by adding 200µL FACS buffer, centrifugation for 4min at 400g at 4°C and removal of the solvent. 100µL fix/perm was added per well and the samples were incubated for 45min at RT. The plate was centrifuged at 400g for 5min. The medium was discarded and the cells were suspended in 100µL FACS buffer before transfer to a FACS tube. The samples were stored in the fridge to analyse the next day with flow cytometry.

Table 4. Amount of pmax GFP DNA and C4SQ10K12 added as VLPs to DCs with a different pre-treatment. SL=sialyl lactose, LPS=lipopolysaccharide and vit D3=vitamin D3.

pDNA (ng)	Protein (µg)	Pre-treatment
27.7	1.38	-
27.7	1.38	SL mix
27.7	1.38	3SL
27.7	1.38	6SL
27.7	1.38	LPS
27.7	1.38	Vit D3

Table 5. Amount of pmax GFP DNA and C4SQ10K12 added as VLPs to DCs with no pre-treatment or SL mix pre-treatment.

pDNA (ng)	Protein (µg)	Sample volume (µL)
30	0.9	1.5
60	1.8	3.0
120	3.6	5.9
30	1.8	2.4
60	3.6	4.8
120	7.2	9.5

6.13.5 Transfection 5: time-dependent formation of VLPs

A fifth transfection was performed for which the time of particle formation was varied. A sample of the immature VLPs was added at t= 45min, 1 h 15min, 2h and 4h. Lipofectamine-plasmid complexes were made according to optimized conditions. The lipoplexes were incubated for approximately 0.5h. The lipoplexes and naked pDNA were added at the same time as t=45min. Before adding each sample, the medium was removed and the cells were washed with 1mL Opti-MEM. The samples were mixed with Opti-MEM prior to adding to the cells. For one series, the samples were removed by taking off all the medium after 3 hour and adding 1mL FCS containing medium (supplemented with 2µL normicin per 1mL). For the other series, the samples were diluted by adding 1mL FCS containing medium (supplemented with 2µL normicin per 1mL) after 3 hours. The HeLa cells were incubated for 48hours at 37°C in a humidified atmosphere with 5% CO_2. The cells were checked for green fluorescence with fluorescence microscopy and analysed with flow cytometry.

Table 6. Amounts of protein and pmax GFP DNA added as VLPs

Incubation of complexes (min)	Sample volume (µL)	Protein (µg)	pDNA (ng)
45	4.76	3.6	60
75	4.76	3.6	60
120	4.76	3.6	60
240	4.76	3.6	60

6.13.6 Transfection 6: delivery of eGFP mRNA

A sixth transfection was performed to test the expression of mRNA. VLPs at ratio N/P= 3 and N/P=6 were made for both the unmodified and the fluorescently labelled protein. Furthermore, the modified protein was also used for VLPs packing pDNA at N/P=3 and N/P=6 and without any genetic material. Lipofectamine-plasmid complexes were made according to optimized conditions. Medium was removed from the cells, washed once with 1mL warm Opti-MEM and prior to adding samples were mixed with Opti-MEM to reach a final volume of 300µL. The cells were incubated for 4 hours at 37°C in a humidified atmosphere

with 5% CO_2. The cells were scanned for green fluorescence with fluorescence microscopy and analysed with flow cytometry.

Table 7. Amounts of protein and eGFP mRNA added at ratio N/P= 3 and N/P=6 as VLPs. The protein is either fluorescently labelled or unmodified.

Sample volume(µL)	Protein (µg)	mRNA (ng)
3.9	0.9	30
7.8	1.8	60
15.6	3.6	120
4.8	1.8	30
9.6	3.6	60
19.2	7.2	120

6.13.7 Transfection 7: RGD labelled protein and pDNA

A transfection was performed for VLPs made out of RGD labelled protein and pDNA at N/P=3 and N/P=6. Lipofectamine-plasmid complexes were made according to optimized conditions. Medium was removed from the cells, washed once with 1mL warm Opti-MEM and prior to adding samples were mixed with Opti-MEM to reach a final volume of 300µL. The cells were incubated for 48 hours at 37°C in a humidified atmosphere with 5% CO_2. After 48 hours, the cells were scanned for green fluorescence with fluorescence microscopy and subsequently analysed with flow cytometry.

Table 8. Amount of RGD labelled protein and pDNA added as VLPs.

Sample volume (µL)	N/P	Protein (ng)	pDNA (ng)
1.5	3	0.9	30
3.0	3	1.8	60
5.9	3	3.6	120
11.8	3	7.2	240
23.6	3	14.4	480
47.3	3	28.8	960
2.4	6	1.8	30
4.8	6	3.6	60
9.5	6	7.2	120
19.0	6	14.4	240
38.0	6	28.8	480
76.1	6	57.6	960

6.13.8 Transfection 8: RGD labelled protein and mRNA

A transfection was performed for VLPs made out of RGD labelled protein and mRNA at N/P=3 and N/P=6. Lipofectamine-plasmid complexes were made according to optimized conditions. Medium was removed from the cells, washed once with 1mL warm Opti-MEM and prior to adding samples were mixed with Opti-MEM to reach a final volume of 300µL. The cells were incubated for 4 hours at 37°C in a humidified atmosphere with 5% CO_2. After 4 hours, the cells were scanned for green fluorescence with fluorescence microscopy and subsequently analysed with flow cytometry.

Table 9. Amount of RGD labelled protein and mRNA added as VLPs.

Sample volume (µL)	N/P	Protein (ng)	pDNA (ng)
1.2	3	0.9	30
2.4	3	1.8	60
4.8	3	3.6	120
9.6	3	7.2	240
19.2	3	14.4	480
38.4	3	28.8	960
2.1	6	1.8	30
4.2	6	3.6	60
8.4	6	7.2	120
16.8	6	14.4	240
33.6	6	28.8	480
67.2	6	57.6	960

6.14 Fluorescence microscopy

Fluorescence microscopy was used to visualize transfected cells and the possible fluorescent products, such as the GFP expression and the dye from the coupling. Fluorescence microscopy was performed on a EVOS fluorescence microscope, a digital inverted microscope by Life Technologies. Images were directly saved as .jpg or .tif files.

6.15 Flow cytometry

Flow cytometry was employed to determine the relative amount of GFP expression in cells transfected with complexes. In general, the technique is referred to as FACS (Fluorescence Assisted Cell Sorting), but the cells are not sorted in this case. Cells were prepared by adding 150µL trypsin per well, incubation for several minutes, adding 300µL FCS containing medium and careful suspending. All sample was transferred to a flow cytometry tube for analysis. Measurements were performed on a Becton Dickson FACSCanto flow cytometry. The threshold was set at 100 000 events to analyse as much cells as possible and the GFP was excited at 488nm with the FITC-A (green) channel. The fluorescent label was excited at 582nm with the PE-Texas Red-A (red) channel. Data was analysed with FlowJo software.

6.16 Maturation of DCs

The maturation of DCs upon exposure to VLPs and protein was examined. The first steps of the procedure are similar to Transfection 4. The DCs did not receive any kind of pre-treatment and VLPs (120ng DNA, 3.6µg protein) were added as well as protein only (7.2µL) besides a blanc. All three samples were suspended in their own medium before transferring to a well on ice. 200µL FACS buffer was added and this time the DCs were vigorously suspended before transfer. The plate was centrifuged at 400g for 5 minutes at 4°C. The medium was discarded and the cells were washed with FACS buffer by adding, centrifugation and removal. A stock solution was made of FACS buffer (36µL per sample) and antibodies for CD86 (2µL per sample) and CD83 (2µL per sample). The cells were gently suspended and incubated in the dark for 30 min. Again, the cells were centrifuged and washed. FACS buffer was added to the sample, cells were resuspended and a dead/live staining was performed by adding DRAQ7 (2µL per sample) and subsequent incubation for 5 min in the dark. The three samples were analysed with flow cytometry.

6.17 Restriction plasmid DNA

Plasmid DNA, pmax GFP, was restricted to test if linear DNA gave better transfection efficiency than circular. 21.5µL RNAse free water, 5µL buffer (10x), 0.5µL BSA (100x), 20µL pmax GFP and 3µL NsiI (10u/µL) were mixed and incubated for 1 hour and 50 minutes at 37°C before storing it in the freezer overnight. An agarose gel was made from 39mL TBE 1x and 0.39g agarose and before pouring the gel 4µL SYBR safe was added. The sample was purified by making use of an extraction kit. 50µL sample, 50µL TBE 1x and 300µL QG were mixed and divided over two tubes. The solution was centrifuged at 12000xg for 1 min before adding 700µL PE buffer to each tube. After 2 minutes, the tubes were centrifuged at 12000xg for 1 min, the flow-through discarded and an additional centrifugation at 17900xg for 1 min. Approximately 100ng of restricted and unrestricted plasmid were prepared separately in 5µL RNAse free water. 1µL 6x loading buffer was added and the entire solution was loaded onto the gel that was placed in the running buffer. The gel was run for 30 min (100V, 0.25mA). An UV picture was taken.

6.18 Nanodrop

In order to determine concentrations of small samples, the Nanodrop 1000 was used. The setting protein A280 was chosen, a background set and 1µL sample was measured. The measured concentration was noted.

7 Results and discussion

7.1 Transfection

7.1.1 Transfection 1: initial search for conditions

An initial search for transfection conditions was performed for HEK and HeLa cells. In both cases, VLPs at N/P=3 were added to the cells and the fluorescence was checked with fluorescence microscopy after 24 and 48 hour (Figure 8). In sharp contrast to the lipofectamine transfected cells, there was no fluorescence observed for the artificial viruses. The complexation of the protein and DNA was successful (Figure 9) and therefore other factors for the absent fluorescence for VLPs must be thought of. First of all, the plasmid itself is functional as demonstrated by the positive control, lipofectamine and therefore not considered a possible factor for the lack of GFP expression. Remarkably, the cells did not show there normal stretched morphology, but were grouped in islands. The samples were prepared in milliQ and quite a large volume (60-240µL) was added on top of 1mL medium. Due to the uncompensated addition of the samples, the cells could have received an osmotic shock resulting in a bad morphology and possible toxicity. Another reason for the lack of GFP expression after VLP transfection, might be that the final concentration of VLPs was too low, indicating a concentration-dependent uptake mechanism. With this in mind, we set out to perform a second transfection.

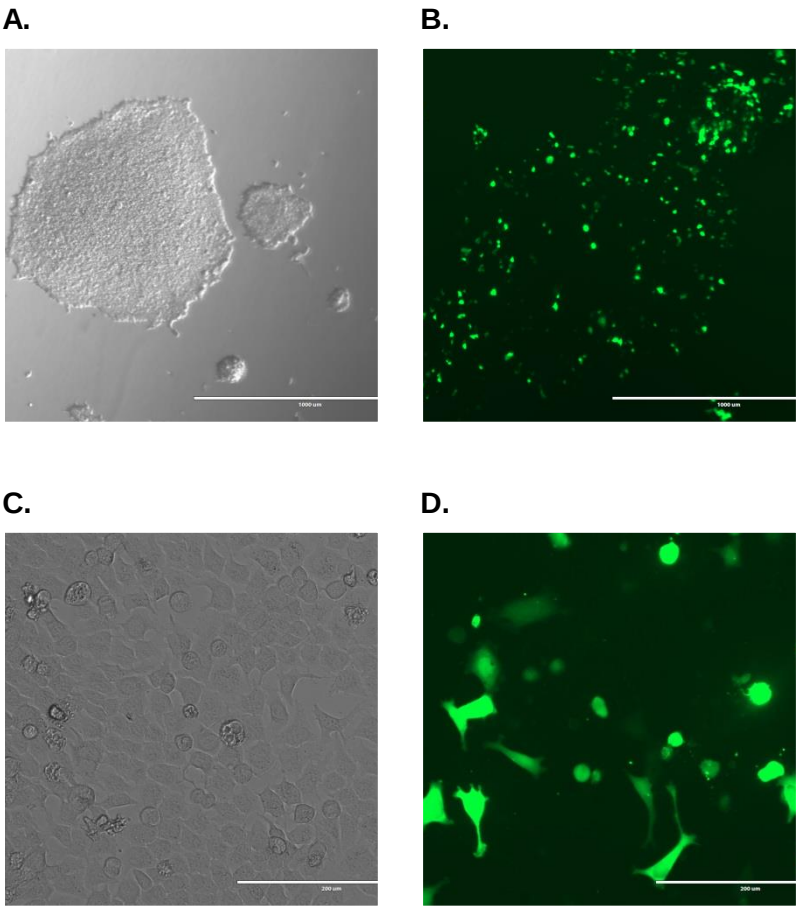

Figure 8. (Fluorescence) microscopy images of HEK and HeLa cells. Scale bar indicates 1000 and 200µm for A, B and C, D respectively. A. Non-treated HEK cells after 24h. B. HEK cells treated with lipofectamine complexes after 24h. C. HeLa cells treated with VLPs after 48h. D. HeLa cells treated with lipofectamine complexes after 48h. The transfection was unsuccessful for the VLPs and successful for the lipoplexes.

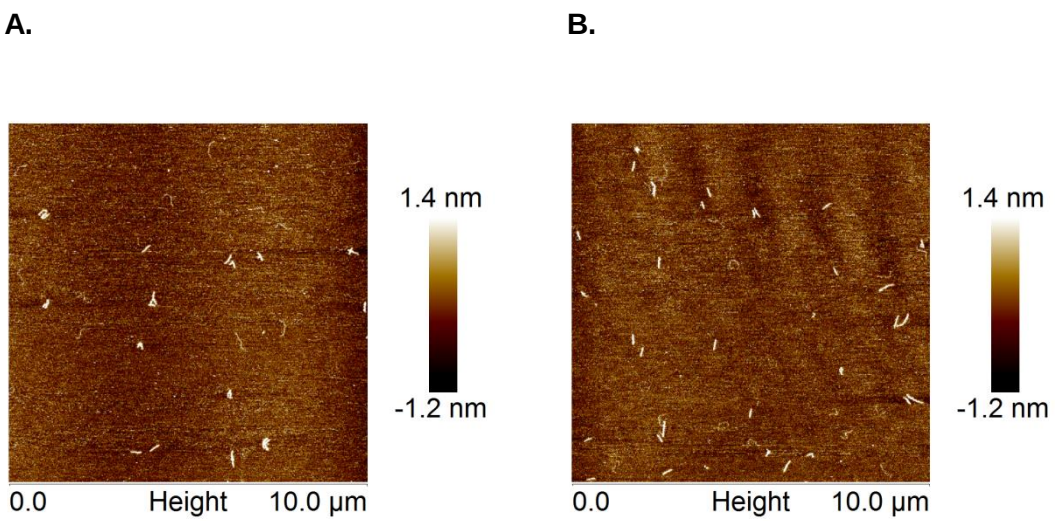

Figure 9. AFM images confirmed the formation of VLPs at N/P=3, which were used to transfect HeLa cells.

7.1.2 Transfection 2: improving transfection conditions

A second transfection with HeLa cells was performed varying several parameters. First, the VLPs were formed either in PB or Opti-MEM as solvent to resemble previously used assembly conditions or compensate for the salt concentration, respectively. Furthermore, the ratio of protein and DNA was varied such that the N/P ratio ranges from approximately 4 to 24. Third, the final concentration of VLPs was increased and the particles were removed after 24 hours and replaced by fresh medium.

For the chosen conditions, some green fluorescent cells were observed! (Figure 10) Already after 24 hours green cells were observed for the whole range of N/P ratios. Interestingly, the HeLa cells treated with complexes formed in Opti-MEM did not show any fluorescence. Although AFM demonstrated the formation of complexes for both solvents (Figure 11 and Figure 12), only the series made in PB showed fluorescence. Therefore, it is hypothesized that the presence of phosphates interacts with the VLPs in a fashion not yet known. Theoretically, the negatively charged phosphate molecules could interact with the positively charged lysines of the K12 or interfere with the hydrogen bonding of the silk domains, SQ10. A possible consequence could be that the proteins loosely pack around the DNA which would make the unpacking of the DNA inside the cell easier and thus overcoming a barrier to delivery. Another hypothesis is that the cells were given an osmotic shock when the PB incubated complexes were applied resulting in an influx of particles. For both complexes formed in PB and Opti-MEM, there was no fluorescence observed when the entire volume on top of the cells constituted only VLP sample. This could be due to the lack of medium and the toxic effect of an osmotic shock given to the cells, because the PB sample was not corrected for salt concentration. Although the transfection was successful, the efficiency of the virus-like particles is not comparable to the efficiency of lipofectamine complexes based on the amount of fluorescence observed with fluorescence microscopy. Having tried several transfection conditions, we next wanted to investigate the influence of the morphology of the plasmid, which can be either circular or linear, on the transfection efficiency.

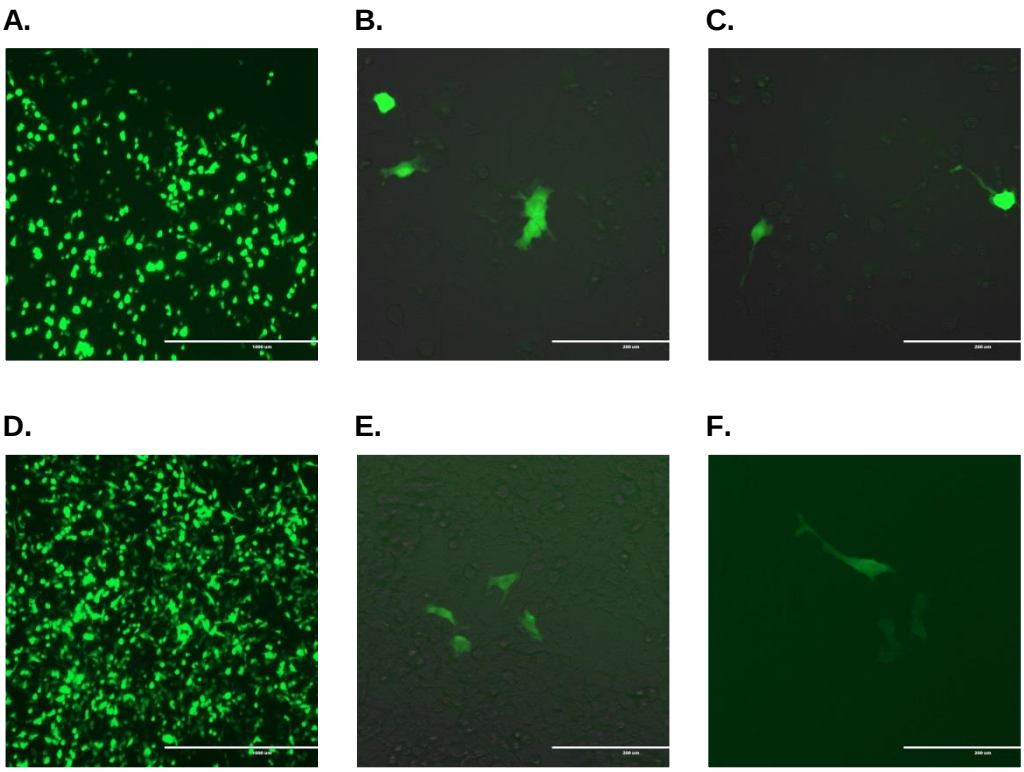

Figure 10. Fluorescence microscopy images of HeLa cells. Scale bar indicates 1000 and 200µm for A, D and B, C, E, F, respectively. A. HeLa cells treated with lipofectamine complexes after 24 hours. B, C. HeLa cells treated with VLPs after 24 hours. D. HeLa cells treated with lipofectamine complexes after 96 hours. E, F. HeLa cells treated with VLPs after 96 hours. Transfection was achieved only for VLPs formed in PB.

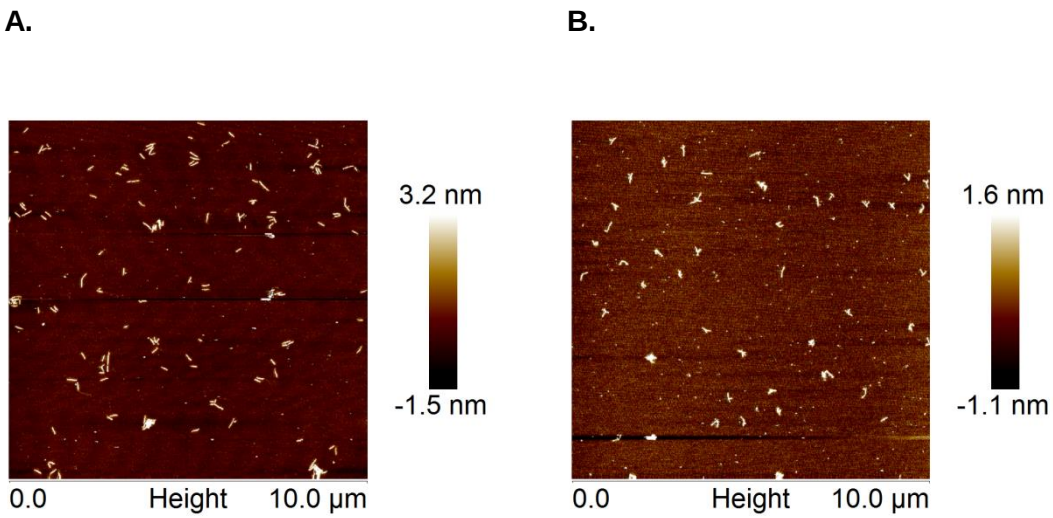

Figure 11. AFM images confirmed the presence of VLPs made in Opti-MEM at different N/P ratios ranging from 4 (A) to 24 (B).

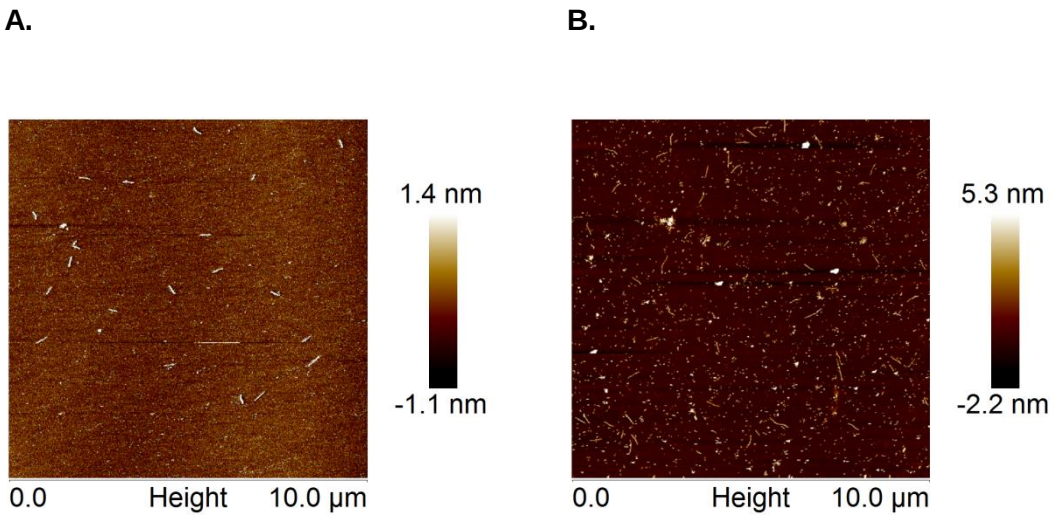

Figure 12. AFM images confirmed the presence of VLPs made in PB at different N/P ratios ranging from 4 (A) to 24 (B). At higher protein concentrations dots appear which could be small protein aggregates.

7.1.3 Transfection 3: linear vs circular

A third transfection was performed with circular or linear plasmids on HEK and HeLa cells. After 24 hour incubation of the VLPs, the salt concentration was corrected by adding PBS in order to prevent osmotic shock. Regrettably, the dilution of the PBS was wrong and therefore higher concentrations, 50x PB and 10x salt, than intended were added. Fluorescence microscopy (Figure 13) indicated very few positive cells as quantitatively confirmed with FACS (Table 10 and Figure 15). Unfortunately, the AFM imaging was not conclusive with regard to particle formation due to technical problems (Figure 14). Therefore the morphology of the VLPs could be an explanation for failed transfection. Besides varying the amount of pDNA, the plasmid was either circular or linear (Figure 35, Appendix). Due to the minimal fluorescence observed with FACS, no conclusions can be made about the transfection efficiency for the presentation of plasmid. Thus far several transfection conditions have been investigated for VLPs containing DNA with HEK and HeLa cells. Therefore a follow-up experiment was performed for a different cell type.

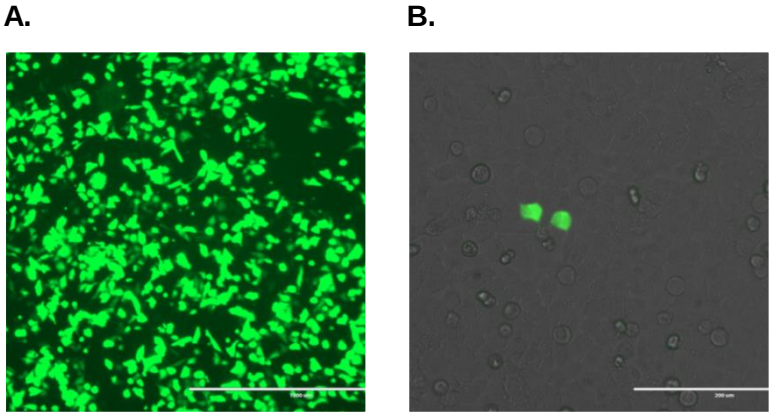

Figure 13. (Fluorescence) microscopy images of HeLa cells. Scale bar indicates 1000 and 200µm for A and B, respectively. A, HeLa cells treated with lipofectamine complexes after 48 hours. B, HeLa cells treated with VLPs after 48 hours.

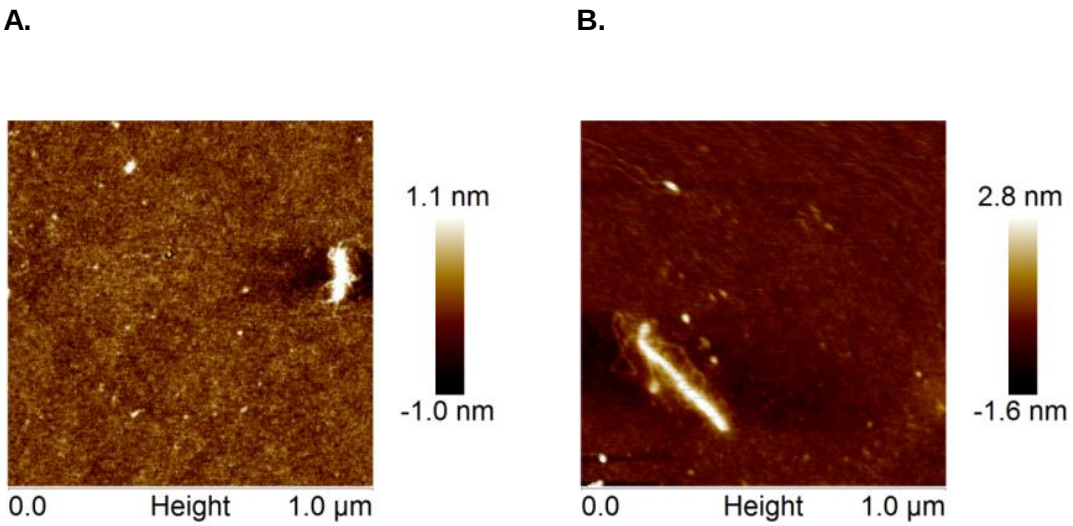

Figure 14. A, B. AFM images of VLPs with N/P=6, which were used to transfect HeLa cells. The particles appear 'ruffled' which could provide an explanation for the failed transfection.

Table 10. FACS data for HEK and HeLa cells treated with VLPs, lipoplexes and medium only. Count indicates all events passing the detector for which the cells are selected (third column) and subsequently the single cells (fourth column). Furthermore, the median is presented and the amount of GFP+ and GFP- cells are given based on the cut-off determined for HEK and HeLa Blanco. Only two values for VLPs (297ng pDNA, highest amount) are shown which were selected for the highest percentage GFP+.

	Count	Cells (%)	Single cells (%)	Median GFP	GFP+ (%)	GFP- (%)
HEK Blanco	11868	43,2	98,7	71.9	0,079	99,9
HEK VLPs	4347	21,1	94,9	80.9	0,81	99,2
HEK Lipoplexes	21712	57,8	99,1	550	58,2	41,8
HeLa Blanco	43677	76,4	98,0	225	0,52	99,5
HeLa VLPs	9108	48,5	94,0	310	2,41	97,6
HeLa Lipoplexes	4393	49,9	91,4	4791	77,4	22,6

A.

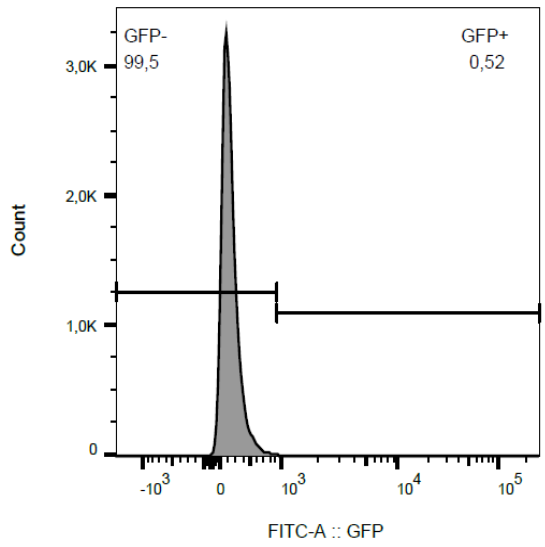

B.

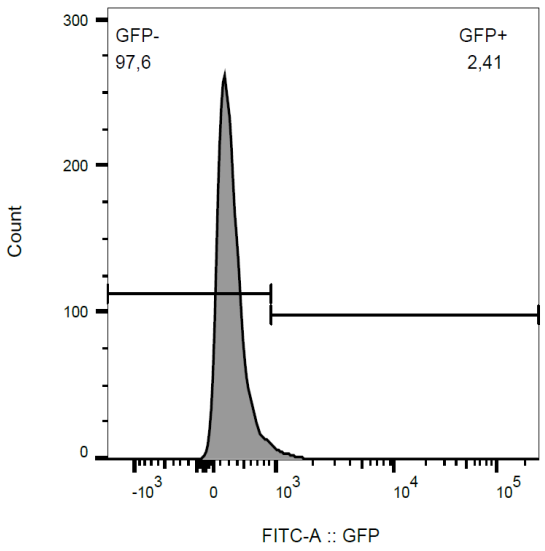

Figure 15. Histogram for HeLa Blanco (A.) and HeLa VLP (B.). The shoulder of the histogram for HeLa cells treated with VLPs increased compared to the blanc indicating minimal GFP expression. However, there is no separate population observed. The FACS data combined with the very few cells imaged with fluorescence microscopy lead to the conclusion that the transfection was not successful.

7.1.4 Transfection 4: dendritic cells

A fourth transfection was performed for dendritic cells, which are professional antigen presenting cells (APCs) and therefore have increased phagocytic activity compared to HeLa and HEK cells. The DCs received different kind of pre-treatments and were subjected to VLPs with ratio N/P=3 or N/P=6 (Figure 16). The amount of GFP expression was analysed with FACS, but the gating was very difficult due to lack of a positive control. Therefore, the amount of GFP+ varies depending on the position of the single cells and the results are not reliable (Figure 17). Moreover, it was very difficult to look for a positive cell with fluorescence microscopy and only one could be detected (Figure 18). Hence, the transfection of DCs was unsuccessful and the phagocytic character of DCs does not influence the transfection efficiency in this case. Therefore, it was decided to switch back to HeLa cells and address the question if the transfection efficiency could be improved by varying the time of assembly for the VLPs.

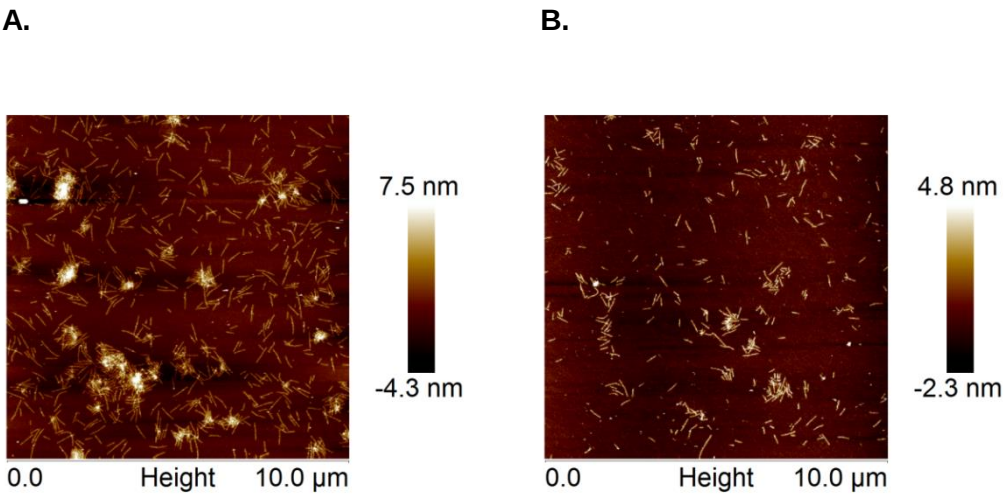

Figure 16. AFM images of VLPs with N/P=6 (A) and N/P=3 (B), which were used to transfect DCs.

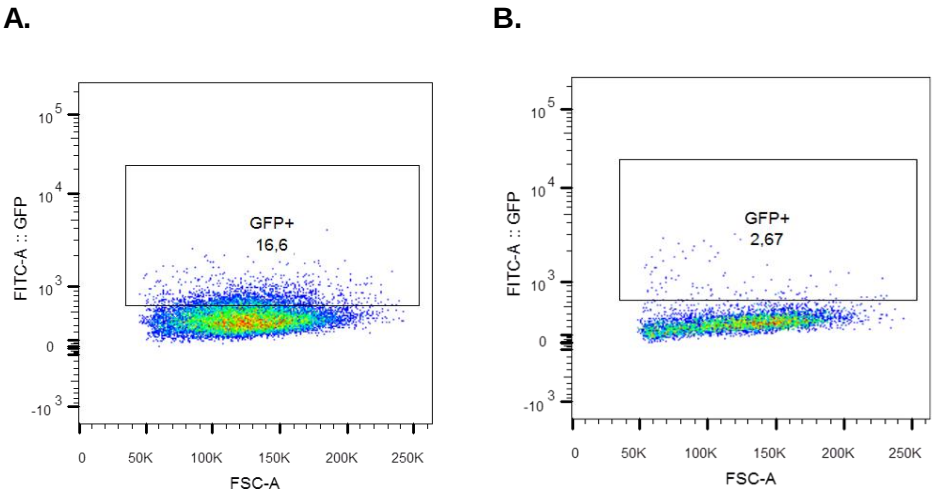

Figure 17. FACS images of DCs treated with VLPs (A) and a blanc (B). The gating for GFP+ is set based on the blanc. In case the entire cell population is increased compared to the blanc, more data points are marked as GFP+, but these could be false positive.

A. B.

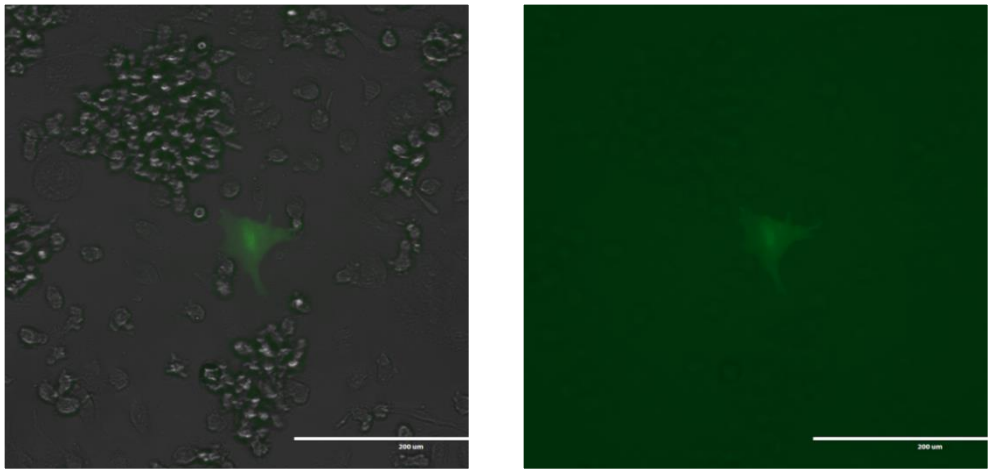

Figure 18. (Fluorescence) microscopy image of one DC. Scale bar indicates 200µm. A. Overlay of fluorescence and bright field image. B. Fluorescence image only.

7.1.5 Transfection 5: time-dependent formation of VLPs

A transfection was performed for which the time of particle formation was varied. Previously, Hernandez-Garcia et al.[13] incubated the complexes only for 1 hour before adding the VLPs to the cell. As noted, the packaging of the DNA might not be complete after a short incubation time and this might influence the transfection. Therefore, we sought to investigate the dependence of the packaging time on the transfection capability. In short, there was no GFP expression observed for particles which were incubated for 0.5h to 4h (Table 11). Misleading, the samples for t=0.5h, 1h and 2h which were not removed have a slightly higher GFP+, but the count is considerably lower than all other samples. Thus far transfection with DNA did not show significant GFP expression, so another experiment was tried with mRNA instead.

Table 11. FACS data for HeLa cells treated with VLPs, lipoplexes and medium only. Count indicates all events passing the detector for which the cells are selected (third column). Furthermore, the median is presented and the amount of GFP+ and GFP- cells are given based on the cut-off determined for HeLa Blanco.

	Sample	Count	Cells (%)	Median GFP	GFP+ (%)	GFP- (%)
No removal	0.5h	9629	17,0	639	1,28	98,7
	1h	14731	30,5	552	0,56	99,4
	2h	12113	27,7	590	0,86	99,1
	4h	95173	56,2	420	0,21	99,8
	Naked pDNA	77746	60,2	424	0,27	99,7
	Lipoplexes	51247	38,9	2578	63,9	36,1
Removal	0.5h	84988	47,2	426	0,18	99,8
	1h	93689	59,6	374	0,099	99,9
	2h	73648	61,8	389	0,15	99,8
	4h	120773	54,4	410	0,13	99,9
	Naked pDNA	83821	56,4	407	0,14	99,9
	Lipoplexes	50627	51,1	1615	50,5	49,5

PB incubated	0.5h	106291	42,6	480	0,37	99,6
	1h	88255	46,5	454	0,24	99,8
	2h	65178	41,1	457	0,27	99,7
	4h	109543	43,5	443	0,24	99,8
Blanc	Blanc	84379	51,5	406	0,21	99,8
	Blanc	73866	55,0	423	0,17	99,8

7.1.6 Transfection 6: delivery of eGFP mRNA

In a previous study, the transfection for VLPs carrying eGFP mRNA was investigated.[44, 45] In order to reproduce the results, different amounts of mRNA and unmodified protein were used to form VLPs and to transfect HeLa cells. The FACS data indicated no GFP expression while the lipoplexes, formed also with mRNA did show GFP expression (Table 12). Although the GFP expression for mRNA was considerably lower than for pDNA, the positive control did indicate that the genetic material was still intact and therefore it was concluded that the delivery of eGFP mRNA with VLPs was unsuccessful.

Table 12. FACS data for HeLa cells treated with VLPs, lipoplexes and medium only. Count indicates all events passing the detector for which the cells are selected (second column). Furthermore, the median is presented and the amount of GFP+ and GFP- cells are given based on the cut-off determined for HeLa Blanco.

Sample	Count	Cells %	Median GFP	GFP+ (%)	GFP- (%)
Blanc	56353	73,1	657	0,63	99,4
Blanc	54477	71,7	661	0,67	99,3
VLPs, N/P=3	85294	81,5	642	0,52	99,5
VLPs, N/P=3	71592	78,6	646	0,58	99,4
VLPs, N/P=3	49408	73,9	606	0,47	99,5
VLPs, N/P=6	78713	80,6	646	0,64	99,4
VLPs, N/P=6	79288	79,8	638	0,55	99,4
VLPs, N/P=6	54385	69,6	617	0,60	99,4
Lipoplexes	96097	64,1	948	9,84	90,2
Lipoplexes	81637	62,3	968	9,57	90,4

7.1.7 Discussion about the delivery of DNA vs RNA

Extensive research has been done on the transfection with VLPs carrying mRNA.[44, 45] In contrast to the experiments with DNA as described here, the previous experiments with mRNA indicated GFP expression and therefore successful transfection. This short discussion focusses on possible pitfalls for the delivery of DNA based on literature, which could provide a possible explanation for the difference between experimental results previously obtained with mRNA and the results for DNA described in this thesis. Although many barriers towards delivery are identical despite the type of cargo, the gene expression of DNA presents additional hurdles which could explain the diminished transfection efficiency for VLPs consisting of DNA and protein (Figure 19). For instance, both RNA and DNA form rod-like structures with the protein C4SQ10K12, but the packing could be different due to the double stranded nature of the DNA. Here we will discuss some of the hurdles DNA faces starting from the naked material inside the cytoplasm and thereby assuming that the delivery route for polynucleotides is the same until that point. Once inside the cytoplasm transport can take place passively via diffusion or actively via directed movement.[46] The diffusion of DNA depends on the size of the fragment, as demonstrated by Lukacs et al.[47] They injected several lengths of double stranded, fluorescein-labelled DNA into HeLa cells and studied the diffusion by fluorescence recovery after photobleaching (FRAP). The diffusion in the cytoplasm decreased over a hundred fold compared to diffusion in water for fragments larger

than 2000bp.[47] Since pmax GFP has a length of circa 3500bp passive diffusion would not suffice for transfection levels comparable to lipofectamine. An alternative for passive diffusion is active transport which takes place along the microtubules for DNA, as investigated by Vaughan and Dean.[48] Furthermore, it was demonstrated that PEI-DNA complexes move along microtubules.[49] Interestingly, transport along the cytoskeleton is boosted by a nuclear localization signal (NLS). This could indicate a dual role of the NLS: loading of the DNA onto the transporter proteins of the microtubule network and active transport into the nucleus. Due to the large size of a typical plasmid diffusion into the nucleus is not possible and therefore active transport with the aid of a nuclear localization signal becomes essential.[46] It is not known for the pmax GFP if a NLS is incorporated. However, in case of absence this would also influence the positive control, consisting of pmax GFP and lipofectamine which still clearly indicates expression of the plasmid and therefore successful delivery. Yet, the additional barriers presented for the delivery of DNA could point to several factors causing diminished transfection. Theoretically, only 0.4% of the naked DNA is intact after 24 hours for an assumed half-life of 3 hours. Moreover, of the material that is delivered inside the cell only 1% reaches the nucleus.[46] Alternatively, for PEI-DNA complexes only 20% of the cells give expression, while the vectors are present in the lysosomes of most cells.[17] This emphasizes that endosomal escape and transport to the nucleus are limiting factors. Likewise, these same factors could be the major hurdles for the gene expression of DNA delivered by VLPs.

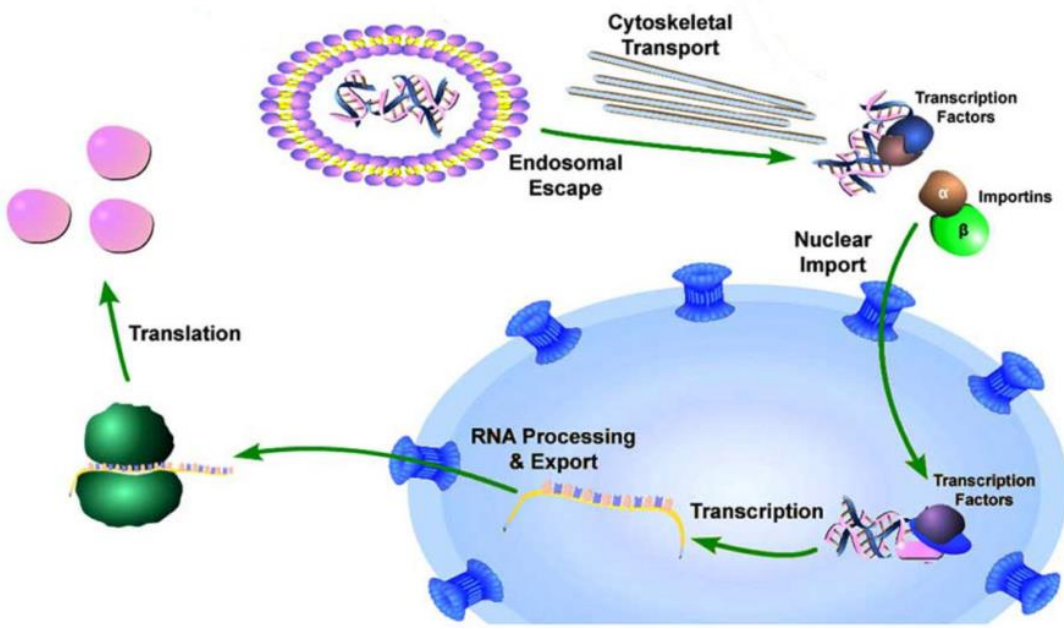

Figure 19. Delivery of DNA has additional barriers including the transport through the cytoplasm to the nucleus and nuclear import. These barriers could limit the transfection efficiency of VLPs carrying DNA. Adapted from Vaughan et al.[46]

7.2 Labelling

The transfection efficiency for the 'naked' VLPs was very low, but through modification of the particle its properties can be altered. Therefore, modification creates a possibility to study the VLPs and especially the reason for low transfection efficiency. The protein C4SQ10K12 was fluorescently labelled with Alexa Fluor 594 in order to test the maleimide-cysteine coupling and furthermore to use the modified protein in a transfection study. Analysis of the chemical reaction was performed with SDS-PAGE, MALDI-TOF and UV/VIS. In addition to the fluorescent labelling, a conjugation with a peptide containing an RGD sequence was performed. Yet, prior to labelling the protein we sought to discover disassembly conditions to disassemble any formed aggregates during the reaction time of the labelling.

7.2.1 Disassembly

Due to the hydrogen bonding of the silk domain, the protein C4SQ10K12 aggregates over time thereby forming small clusters and above the CAC even rod-like structures. We sought for disassembly conditions for the small aggregates and tested urea and the chaotropic salt LiBr.[18] [19] Furthermore, a protein sample was heated, because during sample preparation for VLPs the sample is also shortly heated. Unfortunately, DLS could not be used to study disassembly, because individual monomers could not be distinguished. Therefore, SEC was used instead. Before measuring with SEC, the samples were diluted to a final protein concentration of 0.2mg/mL (Figure 20). The elution profile clearly indicated peaks for the void, dimer and monomer. When the peak for the void is compared qualitatively to the monomer peak an idea can be formed about the ratio of aggregates and monomers. For the tested disassembly conditions the heating at 55°C appears the best method. With disassembly conditions in hand, the chemical coupling and analysis thereof can be performed.

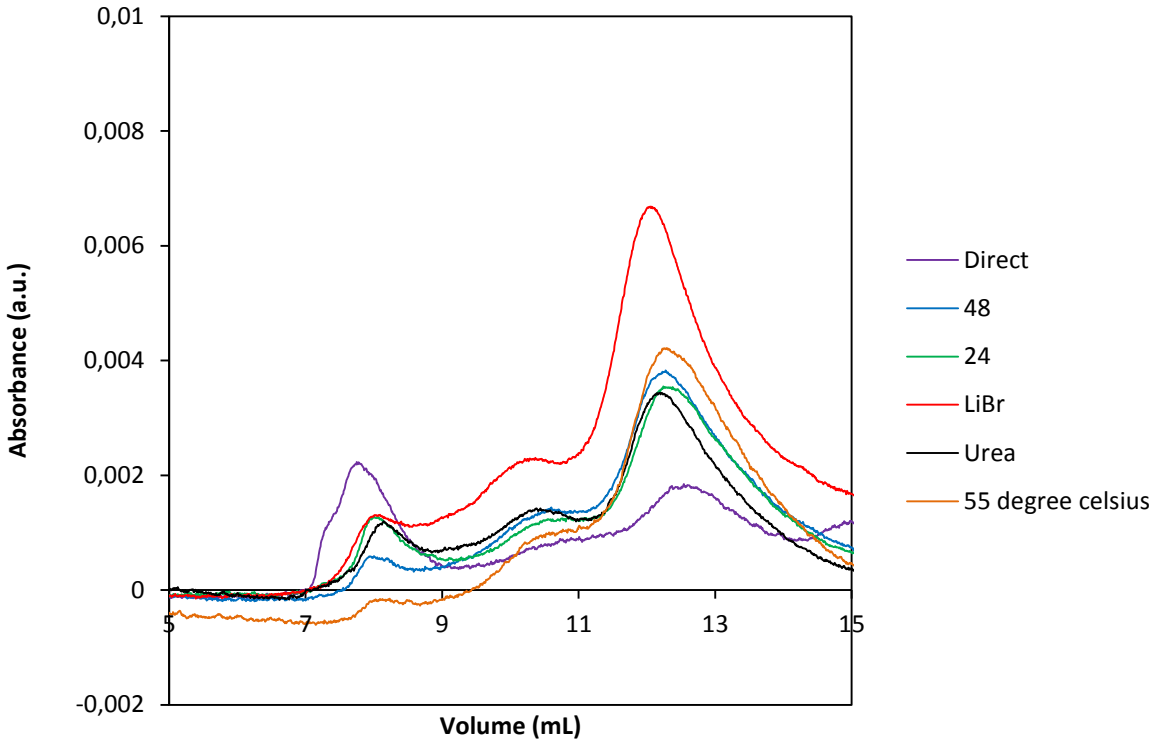

Figure 20. Elution profile of different conditions to disassemble the protein C4SQ10K12. The absorbance was measured at 214nm. Around V=8: void of the column, V=10: dimer and V=12 monomer. The protein solution was measured either directly or after 24 or 48 hours without receiving any treatment. Samples with LiBr or urea were incubated for 24 hours. The best disassembly condition is heating at 55°C for 24 hours.

7.2.2 Analysis of fluorescently labelled protein

Analysis of the coupling started with SDS-PAGE and gel analysis prior to staining revealed a purple band around 100kDa (Figure 21). The protein stain revealed the presence of the modified protein at the same location and therefore it was concluded that the coupling was successful (Figure 22). Moreover, the unmodified protein ran at the same height as the modified protein which only differ 1kDa. Remarkably, the protein mass as determined by mass spectrometry does not correspond to the mass according to gel analysis. This observation has been made previously and can be explained by very hydrophilic nature of the C-block of the protein.[50]

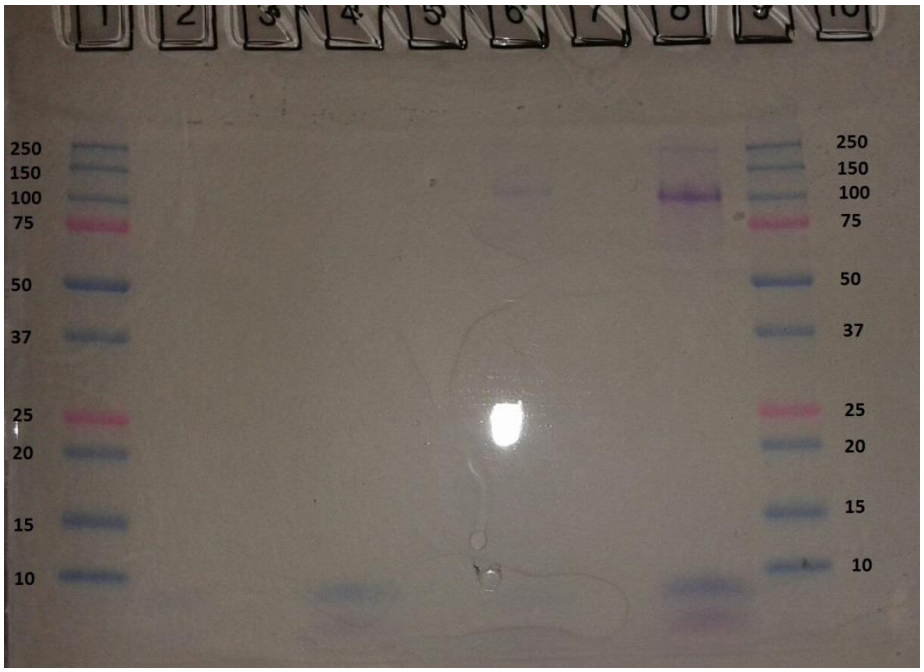

Figure 21. SDS-PAGE prior to staining. Lane 1 and 9: marker, lane 4: unmodified protein and lane 8: modified protein. A purple band is observed around 100kDa indicating fluorescently labelled protein.

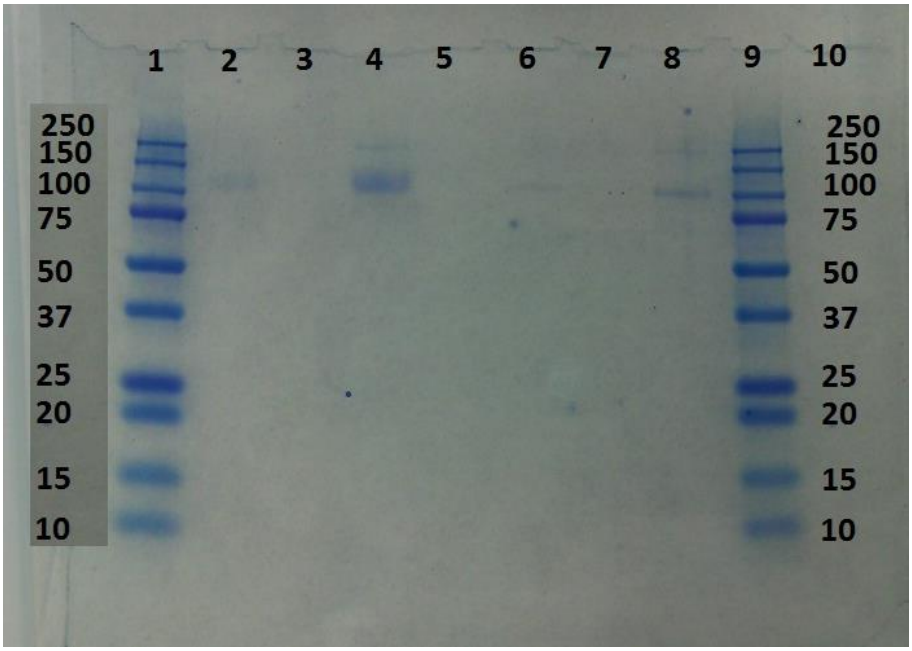

Figure 22. SDS-PAGE after staining. Lane 1 and 9: marker, lane 4: unmodified protein and lane 8: modified protein. Around 100kDa protein is stained which combined with the purple band prior to staining illustrates fluorescently labelled protein.

MALDI-TOF was performed in order to determine the mass of the modified protein (Figure 23). Unfortunately, the mass could not be detected and therefore the chemical coupling could not be confirmed by mass spectrometry.

It was hypothesized that corresponding elution times for the fluorophore and protein would confirm the fluorescent labelling with SEC. Peculiarly, the absorbance at 588nm was non-existing which indicates a technical error (Figure 24). In case the protein was not conjugated to the fluorophore and loose fluorophores would be present, these molecules would have

been detected at a late volume, probably around the solvent change. Because no signal was observed, SEC data was not conclusive about the fluorescent labelling.
UV/VIS was used to assess the labelling degree of fluorescently labelled protein. A calibration curve was made for the dye only (Figure 25). Based on the absorbance of a dilution series of fluorescently labelled protein, the average labelling degree was calculated at 66% (Table 15, Appendix).

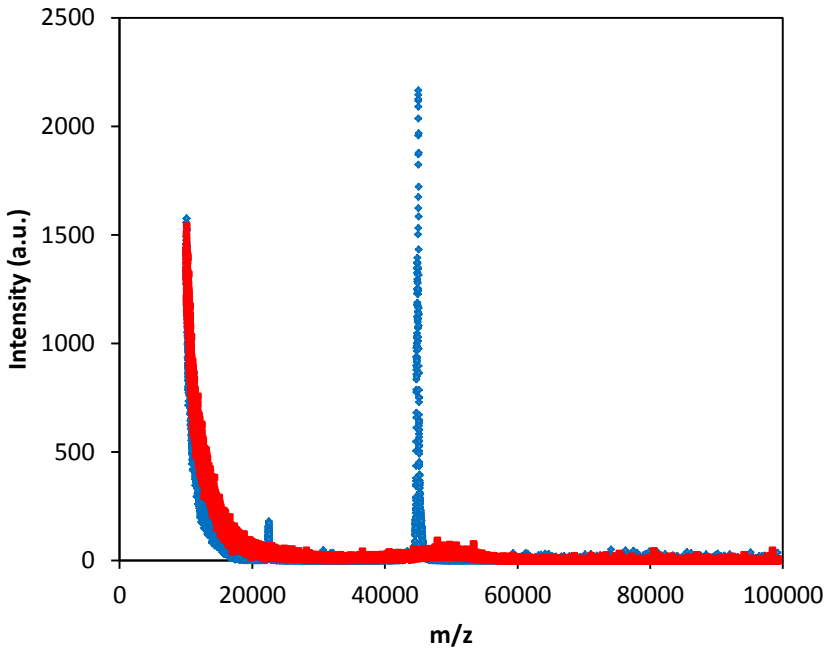

Figure 23. Mass spectrum of unmodified (blue) and modified (red) protein. The protein C4SQ10K12 has a mass of 45058. The fluorescent labelling could not be confirmed with MADLI-TOF.

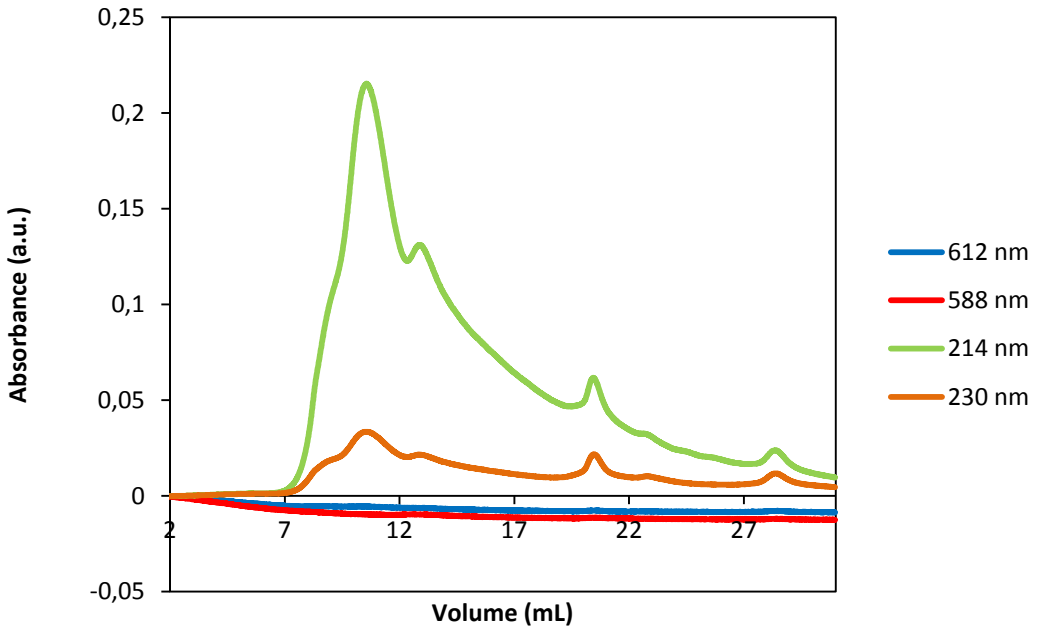

Figure 24. SEC analysis of fluorescently labelled protein after heating for 24hours at 55°C. Due to lack of any signal at 588nm the fluorescent labelling could not be confirmed.

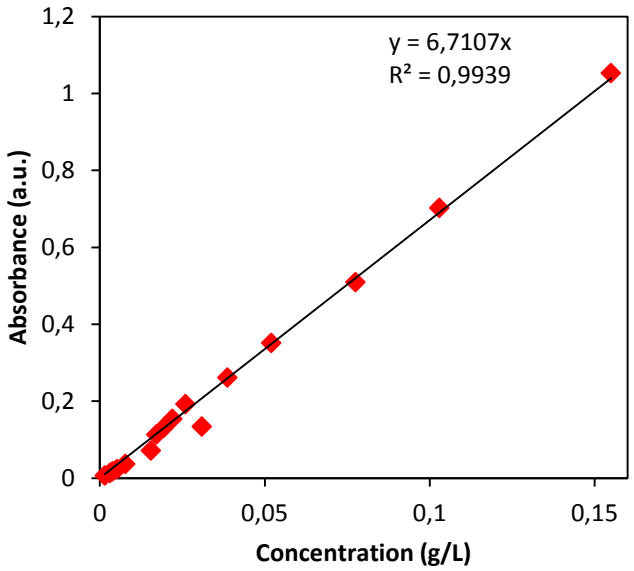

Figure 25. Calibration curve for the fluorescent dye Alexa Fluor 594. A linear correlation was found with an excellent regression.

7.3 Analysis of RGD labelled protein

Besides fluorescently labelling, the protein was also modified with an RGD peptide in a similar fashion as for the fluorophore. A single RGD peptide weighs in our case 851.39Da. When covalently coupled to the C4SQ10K12 protein a mass around 45909Da is expected based on previous measurements of the unmodified protein. However, the observed mass was 45663Da which is roughly 250Da off (Figure 26). Although the result does not seem promising at first sight, the variation for the C4SQ10K12 protein is already quite large itself: 45160Da was reported, which is approximately 100Da different from the data presented in Figure 23. Moreover, the theoretical weight is 44749.2Da and it is known that the variation of the unmodified protein originates from the number of EA repeats.[13] Based on this knowledge and the notable increase of the mass, it is therefore concluded that the protein C4SQ10K12 was successfully labelled with a RGD peptide.

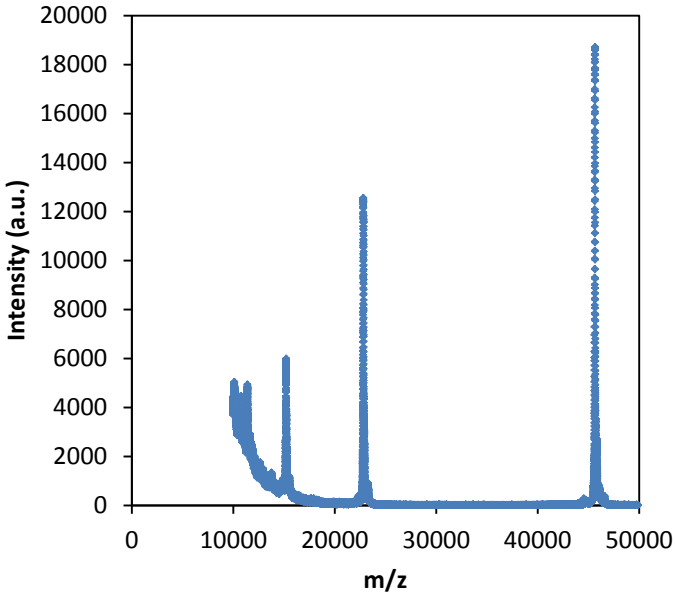

Figure 26. Mass spectrum of RGD labelled C4SQ10K12. The singly ionized peak corresponds to 45663Da, the double ionized peak to 22835Da and the triple ionized peak to 15207Da.

7.4 Tracking the particles

After the successful modification of the protein, the transfection can be studied for VLPs that might have altered properties. So, in addition to the C4SQ10K12 protein, particles with fluorescently labelled protein were formed. Although the VLPs could not be qualitatively checked with AFM nor confocal (Figure 36, Appendix), the FACS data provided an interesting lead about the uptake of the artificial viruses (Table 13). In all cases, the entire cell population shifted for the Alexa Fluor 594+ signal indicating that each cell carries a fluorescent particle in or on the cell. If the presence of fluorophore sticking on the outside of the cell could be ruled out, this finding would point towards successful uptake of the VLPs and an undiscovered hurdle afterwards, for example unpacking or transport of the DNA to the nucleus. Although there could be fluorescent particles on the outer surface instead of inside the cell, flow cytometry proved to be a powerful technique for quantifying the amount of positive cells.

Furthermore, a positive trend was observed for the amount of positive cells and the amount of fluorescently labelled protein (Figure 27). If a single wash is sufficient to remove any sticking protein, uptake of the fluorescently labelled particles was observed. However, for identical amounts of genetic material, but varying N/P ratio's, a discrepancy in the amount of positive cells is noted (Figure 28). Three explanations can be thought of. First, the observed effect originates from the loose protein and for higher ratios there is more loose protein to attach on the cells. Second, the packing density of complexes at N/P=6 is higher and therefore the measured fluorescence intensity is higher than for N/P=3. Third, complexes at N/P=6 have a higher transfection efficiency than particles at N/P=3. Although the different parameters make it impossible to draw definite conclusions from this data set, the experiment illustrates the power of FACS for this transfection study.

Table 13.FACS data for HeLa cells treated with fluorescently labelled VLPs and medium only. Count indicates all events passing the detector for which the cells are selected. Furthermore, the median is presented for Alexa Fluor 594. The amount of Alexa Fluor 594+ and Alexa Fluor 594- are indicated. The amount of GFP+ did not exceed the blanc.

	Modified protein (ng)	Count	Cells (%)	Median Alexa 594	Alexa 594+ (%)	Alexa 594- (%)
HeLa Blanco	0	20857	42,7	579	0,12	99,9
HeLa VLP	2970	174440	69,1	12296	99,3	0,66
HeLa VLP	11880	10904	8,20	27872	98,9	1,12
HeLa VLP	17820	141902	67,7	40054	100,0	0,041

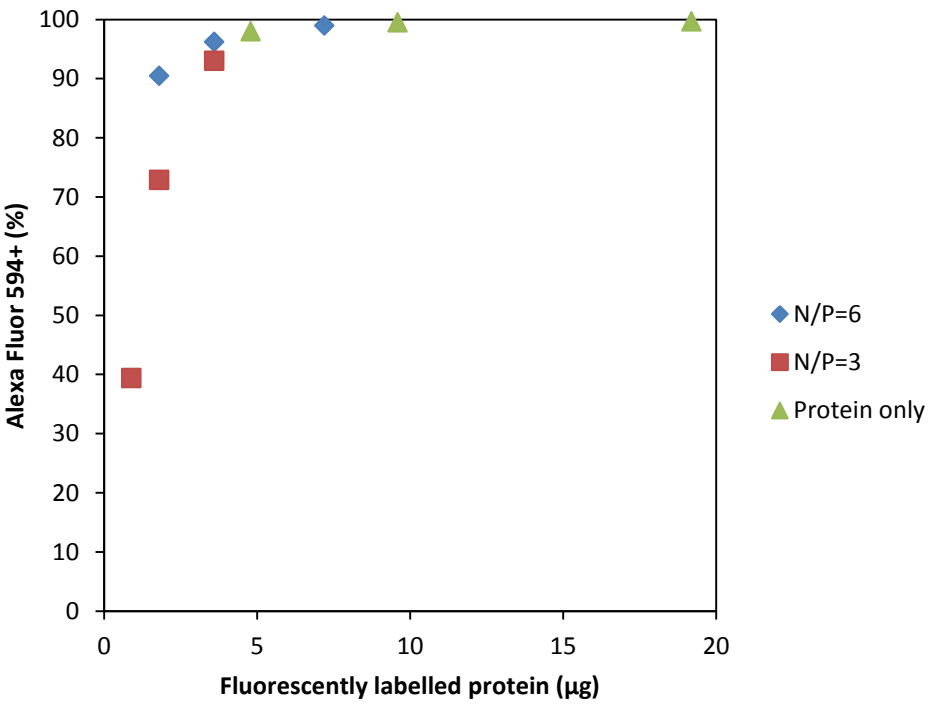

Figure 27. For an increased amount of fluorescently labelled protein, a higher percentage of cells positive for the fluorophore were measured.

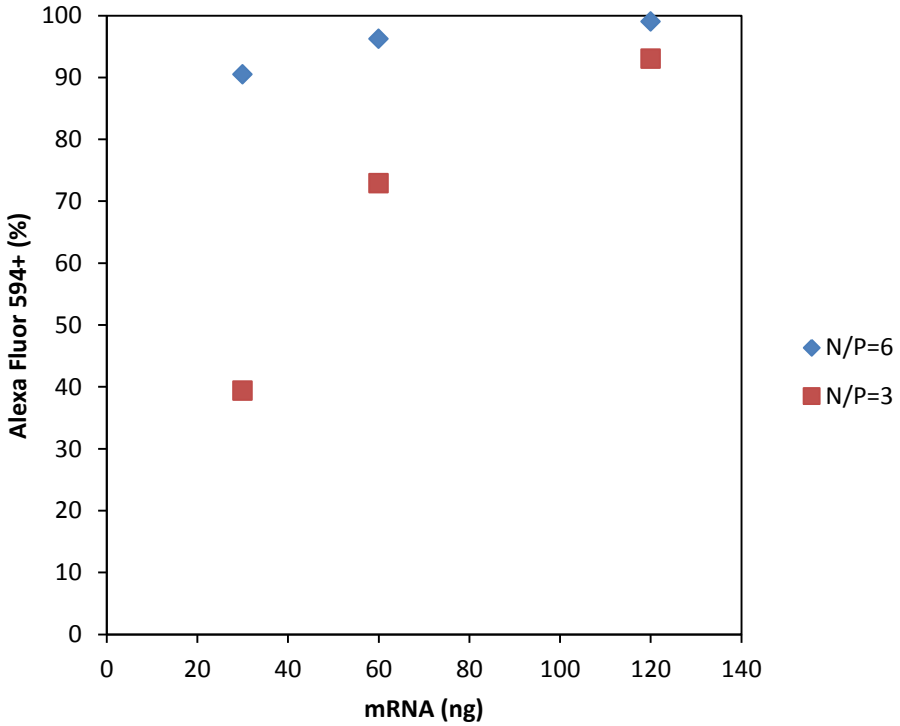

Figure 28. For equal amounts of genetic material different percentages of cells positive for the fluorophore were measured. The discrepancy exists due to the N/P ratio, but cannot be explained conclusively.

7.5 Cell uptake via an adhesion motif

The cellular uptake of particles can be increased by an adhesion motif, in this case an RGD peptide covalently coupled to the C4SQ10K12 protein. VLPs with mRNA or pDNA and the RGD labelled protein were made and used to transfect HeLa cells (Figure 29). Fortunately, some positive cells were observed with fluorescence microscopy for the VLPs containing pDNA (Figure 30). FACS analysis confirmed this observation (Figure 31). Remarkably, most samples had a negligible amount of GFP expressing cells, except for the VLPs with the highest amount of pDNA and N/P=6. One explanation for this could be the increased volume of the sample compared to the other wells causing an osmotic shock. Other reasons could be that particles with N/P=6 have a higher transfection efficiency than particles with N/P=3 or the transfection efficiency depends on the amount of DNA Furthermore, the samples treated with VLPs packing mRNA did not show any significant GFP expression (Table 16, Appendix). Although the number of positive cells was minimal for both DNA and RNA, the few positive cells present were detected with FACS demonstrating the power of this technique. In conjunction with the confirmation of complexation for the RGD labelled protein it was demonstrated that the RGD labelled VLPs successfully transfected a few HeLa cells.

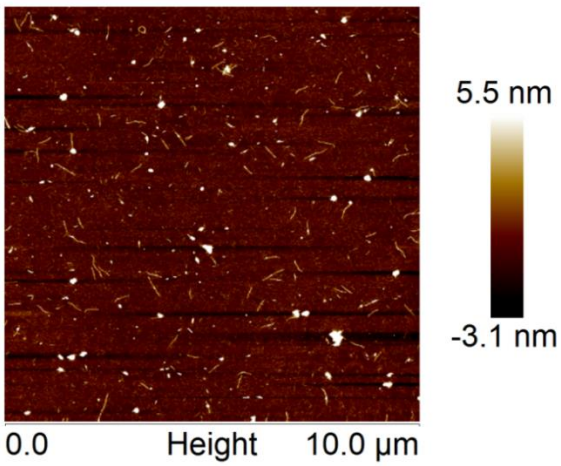

Figure 29. AFM image of VLPs formed out of RGD labelled protein and pDNA at N/P=3.

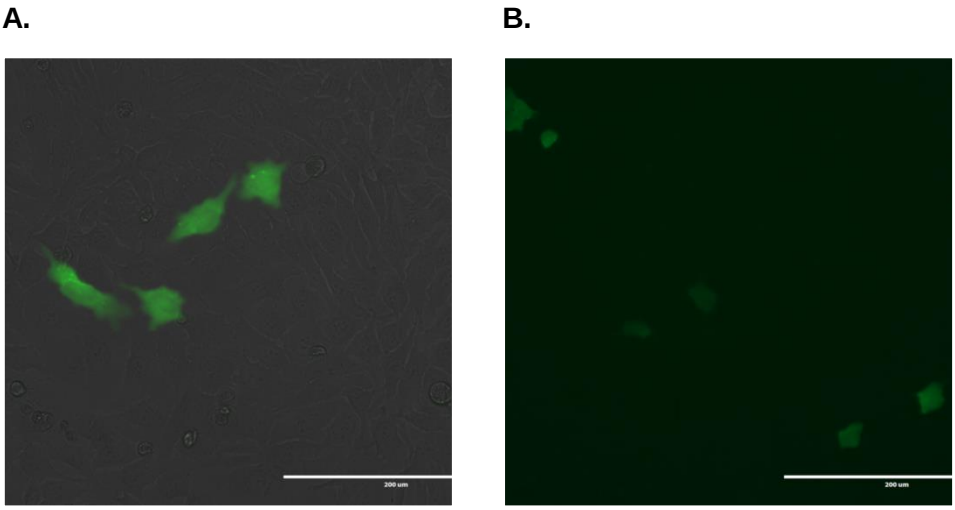

Figure 30. (Fluorescence) microscopy image for HeLa cells expressing GFP after transfection with RGD labelled VLPs carrying pDNA. Scale bar indicates 200µm.

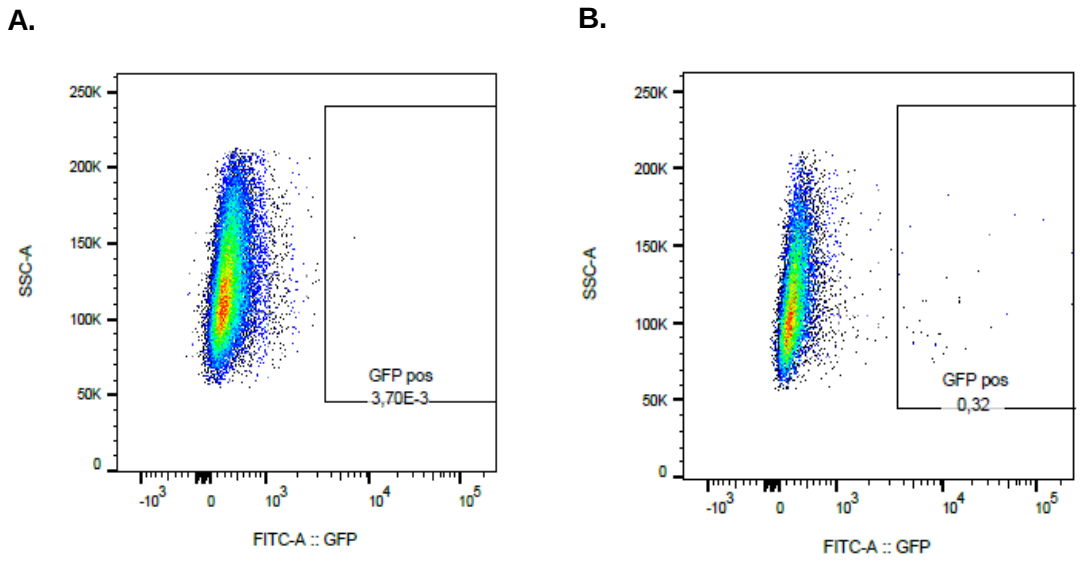

Figure 31. FACS images of HeLa cells non-treated (A) and treated with VLPs containing 960ng pDNA (B). The inset demonstrates that a few cells express GFP when VLPs are added.

Table 14. FACS data for HeLa cells treated with VLPs, lipoplexes and medium only. Count indicates all events passing the detector for which the cells are selected (fourth column). Furthermore, the median is presented and the amount of GFP+ is given based on the inset for HeLa Blanc as shown in the side-scatter GFP plot.

	DNA (ng)	Count	Cells (%)	Median GFP	GFP+ (%)
VLPs, N/P=3	30	36226	36,8	345	0,070
VLPs, N/P=3	60	26826	30,1	335	0,026
VLPs, N/P=3	120	17537	30,2	331	0
VLPs, N/P=3	240	20417	28,0	332	0
VLPs, N/P=3	480	22597	34,0	325	0,027
VLPs, N/P=3	960	25953	34,3	304	0,035
VLPs, N/P=6	30	35251	39,1	351	7,50E-3
VLPs, N/P=6	60	22797	35,5	335	0
VLPs, N/P=6	120	16992	32,1	326	0,019
VLPs, N/P=6	240	32708	36,3	324	0,096
VLPs, N/P=6	480	27890	36,3	306	0,083
VLPs, N/P=6	960	30897	40,2	305	0,32
Blanc	0	55802	50,0	355	3,70E-3
Lipoplexes	500	43338	46,3	2305	42,6

7.6 Maturation of DCs

For the application of the vector it is desirable that the immune system tolerates the VLPs, so multiple administrations are possible. The immunogenicity of VLPs can be tested by measuring the maturation level; for a low maturation level the immune system will tolerate the particles and for a high maturation level an immune response is triggered. The maturation of dendritic cells was analysed with an antibody-mix targeting for CD83 and CD86.[51, 52] The maturation level was determined with a density plot created by FACS. First, the signal for DCs without any antibodies was used to set the gating. Hereafter, a blanc, DCs treated with VLPs (Figure 32), DCs treated with protein only and a positive control were measured (Figure 33). The double positive quadrant indicates a signal for both maturation markers, CD83 and CD86. Compared to the blanc, the VLPs have a higher value for the double positive signal, but a lower value compared to the positive control. Hence, the DCs become mature in the presence of VLPs, but are less stimulated compared to the positive control (LPS). The maturation level of the DCs in the presence of protein is higher than for VLPs, but the amount of protein was two times the amount of protein that was used to assemble the VLPs. From the density plot of the DCs treated with protein, the protein can be ascribed immunostimulatory properties. However, the protein itself could be contaminated with impurities from the production process, for example mannoses and these components could be responsible for the observed immunostimulatory properties of both VLPs and protein.[53]

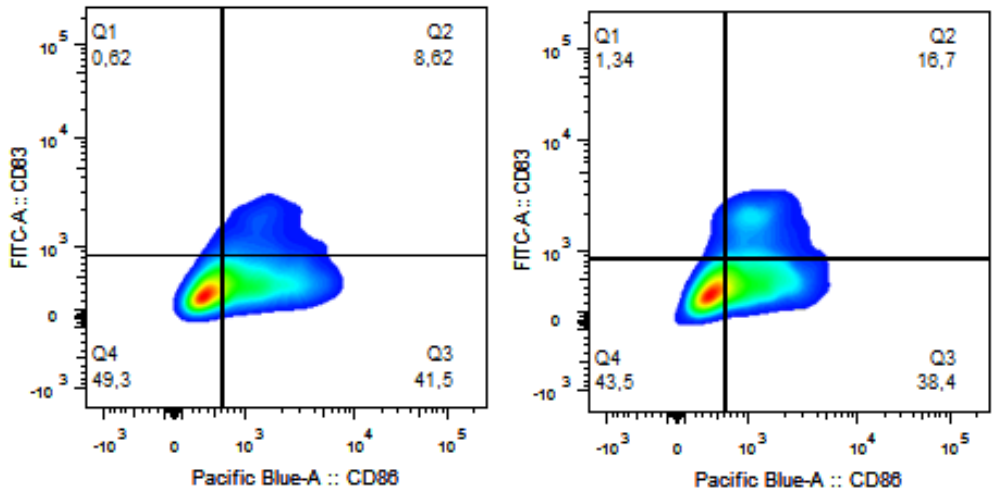

Figure 32. Density plot of FACS data for blanc (left) and DCs treated with VLPs (right).

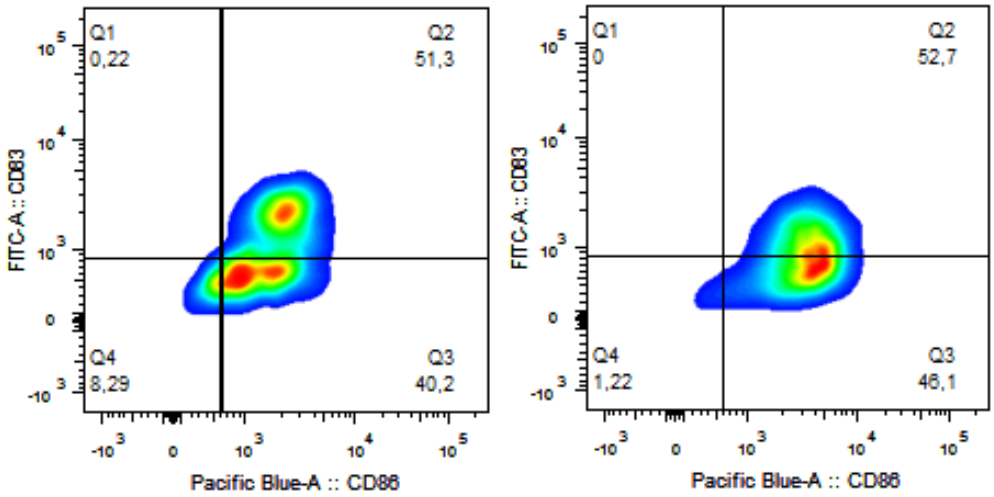

Figure 33. Density plot of FACS data for DCs treated with protein only (left) and a positive control, DCs treated with LPS (right).

8 Conclusion

In conclusion, the barriers towards delivery of genetic material with virus-like particles were successfully explored. Unfortunately, the transfection efficiency of the VLPs could not match the positive control, lipofectamine. However, after conjugation of the fluorophore and peptide to the protein the cell uptake could be studied. Interestingly, this indicated that each cell has taken up a particle pointing to another barrier as the main hurdle. An alternative explanation could be that the fluorescently labelled particles attached on the outside of the cell. If follow-up experiments prove the cell uptake not to be the main hurdle, outstanding candidates are the endosomal escape or unpacking of the VLPs. Furthermore, the few positive cells that were found for the transfection with the RGD modified protein could be analysed by flow cytometry demonstrating the power of this technique. In addition, the immunogenicity of the VLPs was tested with dendritic cells. The data for the maturation of DCs strongly indicates that the maturation level of VLPs is lower than for the positive control and protein only, therefore pointing to tolerance of the VLPs by the body. Importantly, throughout this work a set of techniques, including chemical modification of the C4SQ10K12 protein and analysis of cell uptake by flow cytometry, has been used that could be employed for further studies about the transfection with virus-like particles.

9 Future prospects

This thesis explored some of the hurdles towards successful delivery of genetic material with virus-like particles. For each topic follow-up experiments can be thought of and in particular identifying the barriers for transfection. The fluorescently labelled proteins provided an interesting lead about the uptake of the particles which can be further explored by confocal microscopy. The location of the VLPs on the outside, inside or even the lysosomal compartment in combination with a lysosomal tracker can be studied. Prior to locating the particles, the complex formation of fluorescently labelled protein and genetic material must be confirmed and can be examined with SEM or TEM. Besides confocal microscopy to localize the fluorescent particles, a transfection study blocking various endocytic pathways could be performed to distinguish between active cell uptake or passive attachment of the fluorescently labelled particles on the outside of the cell. Furthermore, endosomal escape as the main barrier can be studied by using mRNA to avoid the nuclear barrier and the peptide GALA to increase the escape from the endosome. In case unpacking of the VLPs is the major hurdle, the amount of free genetic material encoding for GFP can be studied, for example with a dual labelled system or a tag that can isolate the genetic material. Interestingly, the particles formed in phosphate buffer showed some positive cells, but the particles complexed in Opti-MEM did not. Therefore, the effect of phosphate and osmotic shock on the transfection capability could be studied. Ultimately, proteins with different modifications like RGD, fluorophore and GALA can be combined to make an optimized delivery vehicle.

The labelling of the protein can be further fine-tuned by assessing the labelling degree with the Ellman's reagent. The Ellman's reagent quantifies the amount of free thiol spectroscopically and therefore the amount of unreacted protein in the thiol-michael addition.[54, 55]

The immune response towards the protein and the VLPs was tested. However, the protein contained some impurities that could elicit an immune response as well. Therefore, the experiment can be repeated with protein cleaned through ion exchange chromatography and even expanded by studying the cytokine secretion. Additionally, another protein isolated from pichia pastoris can be taken into account to make a comparison with the C4SQ10K12 protein and attribute the immunostimulatory effect definite.

In the long run, a smart design of an artificial virus can be thought of for which different elements are exposed at different time points. A commonly used trick is to use an acid-sensitive element. For instance, the AzMmman linker (Figure 34) is connected to the target molecule and can react with an azide group via a "click" reaction with a helper molecule, like PEG, a dye or a carrier polymer 386. The latter enhances the proton-sponge effect which is a mechanism for endosomal escape. Due to the acid-sensitive nature of the linker, it will be cleaved in the endosome and the target molecule is released. Thus, the linker can assist in reversible PEGylation or endosomal escape.[56] An endosomal escape element provides the opportunity to get one step closer to the ultimate delivery vehicle.

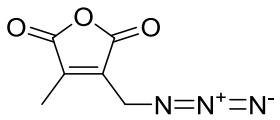

Figure 34. Structure of the AzMmman linker with an azide group for "click" chemistry.

After successful exploration of some of the hurdles towards successful delivery of genetic material with virus-like particles, the main recommendation is to study each barrier in-depth to develop a functional and outstanding delivery vehicle.

10 Acknowledgement

First of all, I would like to thank Renko de Vries for his supervision and providing the protein. Furthermore, thanks to Edwin Tijhaar for his supervision regarding the biologically oriented part. Also thanks to Tom Wennekes for his feedback and tips regarding the chemical part. I would like to thank Wolf Rombouts for his instructions on AFM and image processing, Natalia Domeradzka and Lione Willems for their help with the MALDI-TOF, Inge Storm for her instructions on freeze-drying and tips regarding the SQ10 protein, Mara Winkels-Vink for her quick response via email and ordering of supplies, Remko Fokkink for his instructions on the DLS, Erik van den Brink and Trudi Hermsen for their instructions on cell culturing, Ben Meijer for his help with the FACS and processing of the data, Olaf Perdijk for providing the dendritic cells and antibodies for the maturation experiment and Ties van de Laar and Ruben Higler for their help with confocal microscopy. Finally, I would like to thank Justin Tauber for his support.

11 Reflection on personal learning goals

At the beginning of my thesis I proposed the following personal learning goals:

1. Independently perform research
    a. Conducting experiments
    b. Thinking of experiments
    c. When a problem arises, propose a solution
    d. Critically look at procedures
2. Improving writing skills
    a. Making time to write
    b. Make an outline and think of bridges between sections
    c. Think about careful and concise formulations
    d. Write during the whole thesis
    e. Think of intermediate goals regarding writing and ask for feedback
3. Improving learning
    a. Process feedback
    b. Regular meetings
    c. Midterm evaluation
4. Having fun during presentations
    a. Keep in mind that the audience wants to hear your story and not pin you down

1. Research was performed independently. Experiments were conducted mostly without assistance. During my thesis I experienced a development in designing an experiment. At the start I asked for tips regarding the set-up of an experiment while in the end I could design experiments individually.
2. My writings skills are improved. Although there was not always time to write throughout the thesis there was sufficient time to write. Also, I followed a course for which I wrote a report. This allowed me to practice my writing skills in between and helped me to formulate intermediate learning goals. I think my writing improved, but I would like to keep it as a learning goal in order to pay sufficient attention to it and hopefully become more natural at it.
3. My learning was improved. Feedback on the report, experimental design, practical tips and presentation were processed. Almost every week a meeting was held with at least one of the two supervisors. I found the midterm evaluation very useful, because it gave me insight into the learning process and how my supervisors thought I proceeded.
4. Prior to the presentation I was very nervous, but when I started the presentation the nervousness disappeared. I felt comfortable telling about the work I had done. Also, it helped me to think of the presentation and questions as two different parts. It made me realise that I am not nervous to give a presentation, but answering the question. The questions asked where asked kindly and originated from interest. Practising the presentation for a small audience once before helped me tremendously. Taken altogether I think the presentation was a success and I hope I can think of this experience the next time I am giving a presentation.

Overall, thinking of personal learning goals helped me when the experimental results were not what I was hoping for, because they reminded me that the major goal of a thesis is too master academic skills and not to obtain excellent results.

12 References

1. Sheridan, C., Gene therapy finds its niche. *Nature Biotechnology* **2011,** *29* (2), 121-128.
2. Gilboa, E., DC-based cancer vaccines. *Journal of Clinical Investigation* **2007,** *117* (5), 1195-1203.
3. Grunebach, F.; Muller, M. R.; Brossart, P., New developments in dendritic cell-based vaccinations: RNA translated into clinics. *Cancer Immunology Immunotherapy* **2005,** *54* (6), 517-525.
4. Abbas, A., K; Lichtman, Andrew, H; Pillai, Shiv, *Cellular and Molecular Immunology*. Elsevier: 2015.
5. Kay, M. A., State-of-the-art gene-based therapies: the road ahead. *Nature Reviews Genetics* **2011,** *12* (5), 316-328.
6. Cho, Y. W.; Kim, J. D.; Park, K., Polycation gene delivery systems: escape from endosomes to cytosol. *Journal of Pharmacy and Pharmacology* **2003,** *55* (6), 721-734.
7. Berchel, M.; Le Gall, T.; Couthon-Gourves, H.; Haelters, J.-P.; Montier, T.; Midoux, P.; Lehn, P.; Jaffres, P.-A., Lipophosphonate/lipophosphoramidates: A family of synthetic vectors efficient for gene delivery. *Biochimie* **2012,** *94* (1), 33-41.
8. Lv, H.; Zhang, S.; Wang, B.; Cui, S.; Yan, J., Toxicity of cationic lipids and cationic polymers in gene delivery. *Journal of Controlled Release* **2006,** *114* (1), 100-109.
9. Douglas, K. L., Toward development of artificial viruses for gene therapy: A comparative evaluation of viral and non-viral transfection. *Biotechnology Progress* **2008,** *24* (4), 871-883.
10. Elsabahy, M.; Nazarali, A.; Foldvari, M., Non-Viral Nucleic Acid Delivery: Key Challenges and Future Directions. *Current Drug Delivery* **2011,** *8* (3), 235-244.
11. Gilboa, E.; Vieweg, J., Cancer immunotherapy with mRNA-transfected dendritic cells. *Immunological Reviews* **2004,** *199* (1), 251-263.
12. Geall, A. J.; Verma, A.; Otten, G. R.; Shaw, C. A.; Hekele, A.; Banerjee, K.; Cu, Y.; Beard, C. W.; Brito, L. A.; Krucker, T.; O'Hagan, D. T.; Singh, M.; Mason, P. W.; Valiante, N. M.; Dormitzer, P. R.; Barnett, S. W.; Rappuoli, R.; Ulmer, J. B.; Mandl, C. W., Nonviral delivery of self-amplifying RNA vaccines. *Proceedings of the National Academy of Sciences of the United States of America* **2012,** *109* (36), 14604-14609.
13. Hernandez-Garcia, A.; Kraft, D. J.; Janssen, A. F. J.; Bomans, P. H. H.; Sommerdijk, N. A. J. M.; Thies-Weesie, D. M. E.; Favretto, M. E.; Brock, R.; de Wolf, F. A.; Werten, M. W. T.; van der Schoot, P.; Stuart, M. C.; de Vries, R., Design and self-assembly of simple coat proteins for artificial viruses. *Nature Nanotechnology* **2014,** *9* (9), 698-702.
14. Yin, H.; Kanasty, R. L.; Eltoukhy, A. A.; Vegas, A. J.; Dorkin, J. R.; Anderson, D. G., Non-viral vectors for gene-based therapy. *Nature Reviews Genetics* **2014,** *15* (8), 541-555.
15. Escoffre, J.-M.; Teissie, J.; Rols, M.-P., Gene Transfer: How Can the Biological Barriers Be Overcome? *Journal of Membrane Biology* **2010,** *236* (1), 61-74.
16. Waehler, R.; Russell, S. J.; Curiel, D. T., Engineering targeted viral vectors for gene therapy. *Nature Reviews Genetics* **2007,** *8* (8), 573-587.
17. Bieber, T.; Meissner, W.; Kostin, S.; Niemann, A.; Elsasser, H. P., Intracellular route and transcriptional competence of polyethylenimine-DNA complexes. *Journal of Controlled Release* **2002,** *82* (2-3), 441-454.
18. Rockwood, D. N.; Preda, R. C.; Yucel, T.; Wang, X.; Lovett, M. L.; Kaplan, D. L., Materials fabrication from Bombyx mori silk fibroin. *Nature Protocols* **2011,** *6* (10), 1612-1631.
19. Lammel, A. S.; Hu, X.; Park, S.-H.; Kaplan, D. L.; Scheibel, T. R., Controlling silk fibroin particle features for drug delivery. *Biomaterials* **2010,** *31* (16), 4583-4591.
20. Nair, D. P.; Podgorski, M.; Chatani, S.; Gong, T.; Xi, W.; Fenoli, C. R.; Bowman, C. N., The Thiol-Michael Addition Click Reaction: A Powerful and Widely Used Tool in Materials Chemistry. *Chemistry of Materials* **2014,** *26* (1), 724-744.

21. Kolb, H. C.; Finn, M. G.; Sharpless, K. B., Click chemistry: Diverse chemical function from a few good reactions. *Angewandte Chemie-International Edition* **2001,** *40* (11), 2004-+.
22. Elduque, X.; Sanchez, A.; Sharma, K.; Pedroso, E.; Grandas, A., Protected Maleimide Building Blocks for the Decoration of Peptides, Peptoids, and Peptide Nucleic Acids. *Bioconjugate Chemistry* **2013,** *24* (5), 832-839.
23. Chalker, J. M.; Gunnoo, S. B.; Boutureira, O.; Gerstberger, S. C.; Fernandez-Gonzalez, M.; Bernardes, G. J. L.; Griffin, L.; Hailu, H.; Schofield, C. J.; Davis, B. G., Methods for converting cysteine to dehydroalanine on peptides and proteins. *Chemical Science* **2011,** *2* (9), 1666-1676.
24. Choi, D. S.; Jin, H.-E.; Yoo, S. Y.; Lee, S.-W., Cyclic RGD Peptide Incorporation on Phage Major Coat Proteins for Improved Internalization by HeLa Cells. *Bioconjugate Chemistry* **2014,** *25* (2), 216-223.
25. Choi, K.-m.; Kim, K.; Kwon, I. C.; Kim, I.-S.; Ahn, H. J., Systemic Delivery of siRNA by Chimeric Capsid Protein: Tumor Targeting and RNAi Activity in Vivo. *Molecular Pharmaceutics* **2013,** *10* (1), 18-25.
26. Dal Corso, A.; Caruso, M.; Belvisi, L.; Arosio, D.; Piarulli, U.; Albanese, C.; Gasparri, F.; Marsiglio, A.; Sola, F.; Troiani, S.; Valsasina, B.; Pignataro, L.; Donati, D.; Gennari, C., Synthesis and Biological Evaluation of RGD Peptidomimetic-Paclitaxel Conjugates Bearing Lysosomally Cleavable Linkers. *Chemistry-a European Journal* **2015,** *21* (18), 6921-6929.
27. Ji, S.; Xu, J.; Zhang, B.; Yao, W.; Xu, W.; Wu, W.; Xu, Y.; Wang, H.; Ni, Q.; Hou, H.; Yu, X., RGD-conjugated albumin nanoparticles as a novel delivery vehicle in pancreatic cancer therapy. *Cancer Biology & Therapy* **2012,** *13* (4).
28. Gok, O.; Kosif, I.; Dispinar, T.; Gevrek, T. N.; Sanyal, R.; Sanyal, A., Design and Synthesis of Water-Soluble Multifunctionalizable Thiol-Reactive Polymeric Supports for Cellular Targeting. *Bioconjugate Chemistry* **2015,** *26* (8), 1550-1560.
29. Hersel, U.; Dahmen, C.; Kessler, H., RGD modified polymers: biomaterials for stimulated cell adhesion and beyond. *Biomaterials* **2003,** *24* (24), 4385-4415.
30. Włodarczyk-Biegun, M. K. Silky gels for cells : self-assembling protein-based polymers for use in tissue engineering. Wageningen University, Wageningen, 2016.
31. Sioud, M.; Skorstad, G.; Mobergslien, A.; Sboe-Larssen, S., A novel peptide carrier for efficient targeting of antigens and nucleic acids to dendritic cells. *Faseb Journal* **2013,** *27* (8), 3272-3283.
32. Khalil, I. A.; Kogure, K.; Akita, H.; Harashima, H., Uptake pathways and subsequent intracellular trafficking in nonviral gene delivery. *Pharmacological Reviews* **2006,** *58* (1), 32-45.
33. De Haes, W.; Van Mol, G.; Merlin, C.; De Smedt, S. C.; Vanham, G.; Rejman, J., Internalization of mRNA Lipoplexes by Dendritic Cells. *Molecular Pharmaceutics* **2012,** *9* (10), 2942-2949.
34. Li, W. J.; Nicol, F.; Szoka, F. C., GALA: a designed synthetic pH-responsive amphipathic peptide with applications in drug and gene delivery. *Advanced Drug Delivery Reviews* **2004,** *56* (7), 967-985.
35. Kakudo, T.; Chaki, S.; Futaki, S.; Nakase, I.; Akaji, K.; Kawakami, T.; Maruyama, K.; Kamiya, H.; Harashima, H., Transferrin-modified liposomes equipped with a pH-sensitive fusogenic peptide: An artificial viral-like delivery system. *Biochemistry* **2004,** *43* (19), 5618-5628.
36. Akita, H.; Kogure, K.; Moriguchi, R.; Nakamura, Y.; Higashi, T.; Nakamura, T.; Serada, S.; Fujimoto, M.; Naka, T.; Futaki, S.; Harashima, H., Nanoparticles for ex vivo siRNA delivery to dendritic cells for cancer vaccines: Programmed endosomal escape and dissociation. *Journal of Controlled Release* **2010,** *143* (3), 311-317.
37. Nishimura, Y.; Takeda, K.; Ezawa, R.; Ishii, J.; Ogino, C.; Kondo, A., A display of pH-sensitive fusogenic GALA peptide facilitates endosomal escape from a Bio-nanocapsule via an endocytic uptake pathway. *Journal of Nanobiotechnology* **2014,** *12*.
38. Yamada, Y.; Perez, S. M. V.; Tabata, M.; Abe, J.; Yasuzaki, Y.; Harashima, H., Efficient and High-Speed Transduction of an Antibody into Living Cells Using a

Multifunctional Nanocarrier System to Control Intracellular Trafficking. *Journal of Pharmaceutical Sciences* **2015,** *104* (9), 2845-2854.
39. Koren, E.; Torchilin, V. P., Cell-penetrating peptides: breaking through to the other side. *Trends in Molecular Medicine* **2012,** *18* (7), 385-393.
40. Wadia, J. S.; Stan, R. V.; Dowdy, S. F., Transducible TAT-HA fusogenic peptide enhances escape of TAT-fusion proteins after lipid raft macropinocytosis. *Nature Medicine* **2004,** *10* (3), 310-315.
41. van Bracht, E.; Versteegden, L. R. M.; Stolle, S.; Verdurmen, W. P. R.; Woestenenk, R.; Raave, R.; Hafmans, T.; Oosterwijk, E.; Brock, R.; van Kuppevelt, T. H.; Daamen, W. F., Enhanced Cellular Uptake of Albumin-Based Lyophilisomes when Functionalized with Cell-Penetrating Peptide TAT in HeLa Cells. *Plos One* **2014,** *9* (11).
42. Goswami, D.; Machini, M. T.; Silvestre, D. M.; Nomura, C. S.; Esposito, B. P., Cell Penetrating Peptide (CPP)-Conjugated Desferrioxamine for Enhanced Neuroprotection: Synthesis and in Vitro Evaluation. *Bioconjugate Chemistry* **2014,** *25* (11), 2067-2080.
43. Morris, M. C.; Depollier, J.; Mery, J.; Heitz, F.; Divita, G., A peptide carrier for the delivery of biologically active proteins into mammalian cells. *Nature Biotechnology* **2001,** *19* (12), 1173-1176.
44. Jehkmane, M. Delivery of mRNA using artificial viral coat proteins. Master thesis, Wageningen University, Wageningen, 2015.
45. Haas, R. d. A VLP approach in macromolecular delivery. Wageningen University, Wageningen, 2015.
46. Vaughan, E. E.; DeGiulio, J. V.; Dean, D. A., Intracellular trafficking of plasmids for gene therapy: Mechanisms of cytoplasmic movement and nuclear import. *Current Gene Therapy* **2006,** *6* (6), 671-681.
47. Lukacs, G. L.; Haggie, P.; Seksek, O.; Lechardeur, D.; Freedman, N.; Verkman, A. S., Size-dependent DNA mobility in cytoplasm and nucleus. *Journal of Biological Chemistry* **2000,** *275* (3), 1625-1629.
48. Vaughan, E. E.; Dean, D. A., Intracellular trafficking of plasmids during transfection is mediated by microtubules. *Molecular Therapy* **2006,** *13* (2), 422-428.
49. Bausinger, R.; von Gersdorff, K.; Braeckmans, K.; Ogris, M.; Wagner, E.; Brauchle, C.; Zumbusch, A., The transport of nanosized gene carriers unraveled by live-cell imaging. *Angewandte Chemie-International Edition* **2006,** *45* (10), 1568-1572.
50. García, A. H. Protein-based polymers that Bind to DNA. Wageningen University, Wageningen, 2014.
51. Breloer, M.; Fleischer, B., CD83 regulates lymphocyte maturation, activation and homeostasis. *Trends in Immunology* **2008,** *29* (4), 186-194.
52. Prechtel, A. T.; Steinkasserer, A., CD83: an update on functions and prospects of the maturation marker of dendritic cells. *Archives of Dermatological Research* **2007,** *299* (2), 59-69.
53. Macauley-Patrick, S.; Fazenda, M. L.; McNeil, B.; Harvey, L. M., Heterologous protein production using the Pichia pastoris expression system. *Yeast* **2005,** *22* (4), 249-270.
54. Hansen, R. E.; Winther, J. R., An introduction to methods for analyzing thiols and disulfides: Reactions, reagents, and practical considerations. *Analytical Biochemistry* **2009,** *394* (2), 147-158.
55. Riener, C. K.; Kada, G.; Gruber, H. J., Quick measurement of protein sulfhydryls with Ellman's reagent and with 4,4'-dithiodipyridine. *Analytical and Bioanalytical Chemistry* **2002,** *373* (4-5), 266-276.
56. Maier, K.; Wagner, E., Acid-Labile Traceless Click Linker for Protein Transduction. *Journal of the American Chemical Society* **2012,** *134* (24), 10169-10173.

13 Appendix

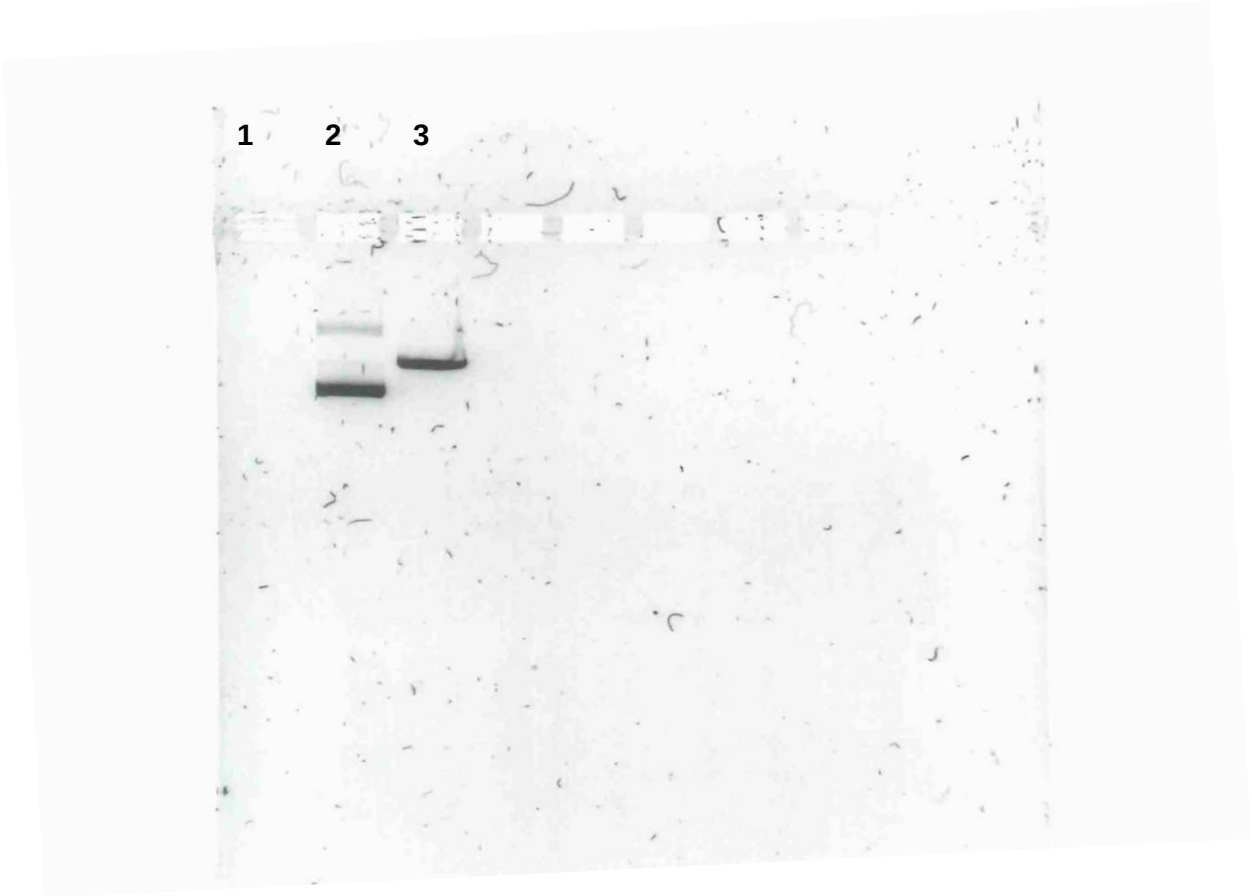

Figure 35. Agarose gel for the analysis of circular and linear plasmid DNA, pmax GFP DNA. Lane 2: unrestricted plasmid. On top is relaxed plasmid and bottom is probably supercoiled plasmid. Lane 3: restricted plasmid. The plasmid was successfully restricted, because there is only a single band present in lane 3.

Table 15. Labelling degree of fluorescently labelled C4SQ10K12. The averaged labelling degree is 66%.

Conc (g/L)	Abs	Calculated conc fluorophore (g/L)	Labelling degree
0.25	1.10	0.16	0.66
0.17	0.74	0.11	0.66
0.13	0.58	0.09	0.69
0.10	0.47	0.07	0.69
0.05	0.22	0.03	0.66
0.03	0.15	0.02	0.66
0.03	0.11	0.02	0.65
0.02	0.08	0.01	0.63
0.01	0.04	0.01	0.66

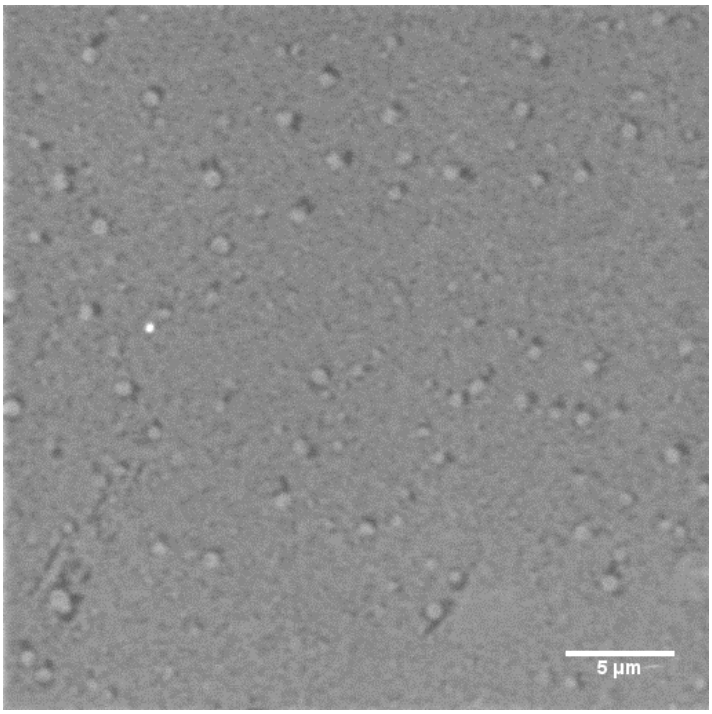

Figure 36. Confocal microscopy image of fluorescently labelled proteins and pDNA. Due to the small size of the complexes they are below spectral resolution. Furthermore, the label was not suited for the set-up, because the lasers available are at 545nm and 630nm while the excitation maximum is around 590nm. The picture shows several larger structures which could be aggregates and some smaller structures at the background. Due to the averaging for making this picture, the small structures cannot be noise. Confocal microscopy could neither confirm or exclude the presence of VLPs and indicated mostly that another technique should be used for confirmation.

Table 16. FACS data for HeLa cells treated with VLPs, lipoplexes and medium only. Count indicates all events passing the detector for which the cells are selected (fourth column). Furthermore, the median is presented and the amount of GFP+ is given based on the inset for HeLa Blanc as shown in the side-scatter GFP plot. Unfortunately, the measurements for mRNA=30 and 960ng, N/P=3 and mRNA=60ng N/P=6 are missing due to technical errors.

	mRNA (ng)	Count	Cells (%)	Median GFP	GFP+ (%)
VLPs, N/P=3	60	28431	55,5	468	0,085
VLPs, N/P=3	120	12238	57,5	467	0,22
VLPs, N/P=3	240	30763	60,6	478	0,11
VLPs, N/P=3	480	28550	55,2	473	0,059
VLPs, N/P=6	30	39064	59,0	497	0,12
VLPs, N/P=6	120	28982	57,5	460	0,080
VLPs, N/P=6	240	37994	60,0	481	0,14
VLPs, N/P=6	480	28003	57,4	441	0,11
VLPs, N/P=6	960	32194	48,9	426	0,046
Lipoplexes	500	20416	53,2	1028	9,18
Lipoplexes	500	48215	47,9	1258	12,6
Blanc	0	42752	54,5	497	0,11
Blanc	0	44795	60,4	531	0,14